

CELL SURVIVAL CHARACTERIZATION OF HUMAN AMNION MESENCHYMAL CELLS
GROWN IN NOVEL 3D CULTURE SYSTEM AND GENE EXPRESSION COMPARISON TO 2D
CULTURE

A THESIS SUBMITTED TO THE GRADUATE DIVISION OF THE
UNIVERSITY OF HAWAI'I AT MĀNOA IN PARTIAL
FULFILLMENT OF THE REQUIREMENTS FOR THE DEGREE OF
MASTER OF SCIENCE

IN
DEVELOPMENTAL AND REPRODUCTIVE BIOLOGY

AUGUST 2015

By
Kimberly A. Foca

Thesis Committee:
Yusuke Marikawa, Chairperson
Claire Wright
Olivier Le Saux

ACKNOWLEDGEMENTS

First and foremost, I would like to share my appreciation for the graduate program of Developmental and Reproductive biology for the opportunity of obtaining my Master's Degree. Each professor encouraged my own growth as a scientist and inspired me with their dedication and passion for the research field. A special admiration and respect for the members of my thesis committee for their vast amount of kindness and support through each aspect of obtaining my degree.

My deepest appreciation to Dr. Claire Wright for all her words of encouragement through my unsuccessful moments ensuring me that it is all part of the process. She gave me the honor of working under her and learn from her vast amount of knowledge to leave a mark in the world of saving babies. I will forever be grateful for all that she has enlightened me with in all my future endeavors. Thank you to everyone in the Dr. Wright lab for your support and ability to make me laugh when I needed it the most. Especially, Dr. Brittany Sato who allowed me to tap into her knowledge and use her immaculate pipettes.

Warmest gratitude for the Department of Anatomy, Biochemistry, and Physiology for supporting me financially through my graduate education with a teaching assistantship. It gave me the chance to share what I learned and help encouraged others to pursue a higher education. I have a deep admiration for Dr. Deborah Merritt who fascinated me daily. Her intense passion and incredible amount of knowledge inspired me and gave me the drive to be as amazing as she is.

Lastly and importantly, I will like to thank my parents, Alfred and Lynn, for their undying love, support, and encouragement. A special thank you to my husband, Douglas, for his patience and insistence that I follow my dreams. Thank you to my friends and classmates for venturing with me through this amazing experience.

TABLE OF CONTENTS

ACKNOWLEDGEMENTS	ii
LIST OF FIGURES	iv
LIST OF ABBREVIATIONS	vi
CHAPTER 1. BACKGROUND	1
1.1 SIGNIFICANCE OF PRETERM BIRTH	1
1.2 RUPTURE OF THE FETAL MEMBRANES	4
1.3 PRETERM PREMATURE RUPTURE OF THE FETAL MEMBRANES	8
1.4 THE USE OF ANIMAL MODELS IN PRETERM BIRTH AND PPRM RESEARCH	9
1.5 THE STRENGTH OF THE FETAL MEMBRANES LIES WITH THE AMNION	11
1.6 COLLAGENS OF THE MESENCHYMAL LAYER AND THE AMNION MESENCHYMAL CELLS	12
1.7 2D CELL CULTURE	13
1.8 3D CELL CULTURE	15
1.9 STUDY PURPOSE	16
CHAPTER 2. SPECIFIC AIM 1	
2.1 INTRODUCTION	18
2.2 AIM 1 CHARACTERIZATION OF A NOVEL AMC 3D CULTURE SYSTEM TO IMPROVE THE UNDERSTANDING OF THE ROLE OF THESE CELLS IN THE AMNION AND ROM	23
2.3 MATERIALS AND METHODS	26
2.4 RESULTS	33
2.5 DISCUSSION	38
CHAPTER 3. SPECIFIC AIM 2	
3.1 INTRODUCTION	62
3.2 GENE EXPRESSION PROFILES OF AMC IN 2D AND 3D	65
3.3 MATERIALS AND METHODS	67
3.4 RESULTS	70
3.5 DISCUSSION	71
CHAPTER 4. DISCUSSION	81
REFERENCES	86

LIST OF FIGURES

Figure 1. Preterm Birth Rate in Hawai'i	2
Figure 2. Layers of the Human Amnion	5
Figure 3. Center of Gravity during Pregnancy	10
Figure 4. Polarity of Cells in 2D and 3D Culture	14
Figure 5. H&E Stain of Human Fetal Membranes	45
Figure 6. Seeding Densities of AMC in Alvetex Scaffold	47
Figure 7. Seeding Density of 400,000 and 500,000 AMC in Alvetex Scaffold	48
Figure 8. Overall Density Study	49
Figure 9. Linear Regression of AMC Cell Density	51
Figure 10. Phalloidin and DAPI Label of AMC in 2D and 3D	52
Figure 11. AMC Resting Within Scaffold Pore	53
Figure 12. Vimentin Label of AMC in 3D	54
Figure 13. H&E Stain of AMC 400,000 Time Course	55
Figure 14. H&E Stain of AMC 500,000 Time Course	56
Figure 15. H&E Stain of AMC Monolayer	57
Figure 16. Quantification of AMC 400,000 Time Courses	58
Figure 17. Quantification of AMC 500,000 Time Courses	59
Figure 18. Propidium Iodide Label of AMC	60
Figure 19. LDH Secretion of AMC in 2D and 3D	61
Figure 20. Relative Gene Expression of AMC in 2D and 3D	80

LIST OF TABLES

Table 1. Quantification of AMC within the Human Fetal Membranes	46
Table 2. Quantification of Complete Cell Density of AMC in Scaffolds	50
Table 3. Quantification of AMC 400,000 and 500,000 Density Studies	50
Table 4. Extracellular Matrix Cell Adhesion Array of AMC in 2D and 3D	75
Table 5. Chosen Genes from PCR Array for qRT-PCR	79
Table 6. Endogenous Gene Expression for qRT-PCR Gene Primers	79

LIST OF ABBREVIATIONS

2D	Two-Dimensional
3D	Three-Dimensional
AEC	amnion epithelial cells
AMC	amnion mesenchymal cells
BMI	body mass index
Ca ²⁺	calcium
CAPs	contraction-associated proteins
cDNA	complementary DNA
CT	cycle threshold
DMEM	Dulbecco's Modified Eagle Medium
ECM	extracellular matrix
FADD	fas-associated protein with death domain
FBS	fetal bovine serum
FN1	fibronectin
HiF-1 α	hypoxia inducible factor 1-alpha
MET	Mesenchymal-epithelial transition
MLCK	myosin light-chain kinase
MMP	matrix metalloproteinase
MTT	mitochondrial dehydrogenase activity
NKB	Nukbone
NO	nitric oxide
PBS	phosphate buffer saline
PCR	polymerase chain reaction
PFA	paraformaldehyde
PGI ₂	prostacyclin
PI	propidium iodide
PPROM	preterm premature rupture of the fetal membranes
PTHrP	parathyroid hormone-related peptide
qRT-PCR	reverse transcriptase real-time polymerase chain reaction
RIPA	radioimmunoprecipitation assay
RNA	ribonucleic acid
RNA-Seq	RNA sequencing
ROM	rupture of the fetal membranes
ROS	reactive oxygen species
SSC	saline sodium citrate
TIMP	tissue inhibitor of metalloproteinase
TNF	tumor necrosis factor
ZAM	zone of altered morphology

Chapter 1. Background

1.1 Significance of Preterm Birth

Preterm birth is defined as the delivery of a baby prior to a gestational age of 37 weeks. The consequences associated with preterm birth are the leading cause of prenatal and neonatal mortality, and account for several morbidities including neurologic handicaps, necrotizing enterocolitis, sepsis, and developmental delay (Bryant-Greenwood, Millar, 2000; Kim *et al.* 2011; Mercer 2004). In the United States, preterm birth occurs at a significantly high rate, between 12-13% affecting about 450,000 babies annually (March of Dimes 2015), this is high compared to other developed nations who have occurrence rates between 5-9% (Goldenberg *et al.* 2008). The reasons for the differences in preterm birth rates between the U.S. and other developed nations remains unknown.

Although much is still not understood about the underlying causality of preterm birth, it is clear that there is an increased incidence of preterm birth between different ethnicities. Overall, African Americans are the ethnic group that experiences the highest prevalence of this disorder (16-18%) in the United States (Goldenberg *et al.* 2008). However, in Hawai'i the African American population is small compared to continental U.S. and this is reflected in the prematurity disparity showing the highest rates in Native Hawaiian and Pacific Islander populations. They also exhibit the highest occurrence of premature infant death in Hawai'i with the second highest overall infant mortality rate at a prevalence of 66% greater than Caucasians (Hirai *et al.* 2013). It was estimated that in 2010 that 1 out of every 10 pregnant women living in Hawai'i suffered from a preterm delivery (Hayes *et al.* 2010), although this constitutes a

significant problem, the Native Hawaiian population is reported to suffer from a rate as high as 55% (Hirai et al. 2013). The rate of preterm birth in Hawai'i has gradually increased to its current 12.2% rate (Figure 1), which ranks the state among one of the highest, along with many southern states (United Health Foundation 2015). The problem of preterm birth is a significant issue for the Native peoples of Hawaii, remaining a tragedy for the future health of one of the few indigenous populations to the United States.

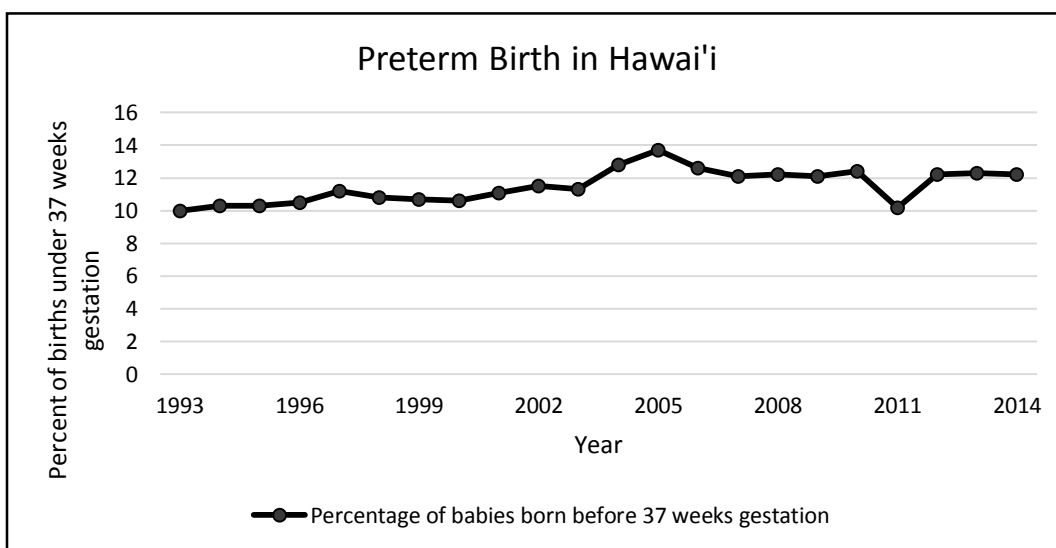


Figure 1. Percentage of preterm birth rate in Hawai'i from 1993-2014. (Adapted from United Health Foundation. *America's health rankings – preterm birth*. 2015. www.americashealthrankings.org/HI/preterm)

The rate of preterm birth overall in the U.S. has remained mostly unchanged since 2001 despite increased risk recognition, (Hayes *et al.* 2010) rendering it an ongoing national problem without a significant resolution. This continuing issue of preterm birth leaves not only the accompanying emotional toll on the families who suffer, but also a large financial burden costing the U.S. health care system over \$26 billion annually (Centers for Disease Control and Prevention 2015). One reason why preterm birth remains a lingering issue is because research in this field has proven difficult due to several inherent issues involved with this kind of work.

One such issue are the ethical constraints, as it is obviously unethical to intervene in human pregnancies due to the serious detrimental ramifications to the mother and unborn child and a noninvasive technique to study preterm birth has yet to be discovered. The cause of preterm birth is currently unknown for many cases, as there is a lack of adequate research methods and differing risks among ethnic groups are compounded by many other social complexities like education and socioeconomic diversity.

Although several risk factors associated with preterm birth have been identified, the US preterm rate remains consistently high. Many of these are centered on poor maternal social decisions that include, tobacco and drug use that diminish fetal oxygen supply, and alcohol consumption, that works as a physical and behavioral teratogen (Hayes *et al.* 2010; Patrinos 2002). The quality of maternal health also contributes to the risk of preterm birth (Hayes *et al.* 2010) as women with a low, or high body mass index (BMI) are at higher risk for spontaneous preterm birth most likely due to nutritional deficiencies, pre-eclampsia, or diabetes (Goldenberg *et al.* 2008). However, not all risks that play into this syndrome are of maternal socioeconomic origin as this syndrome also has a pattern of inheritance. Thus, women who have already experienced a preterm delivery have a 15-50% risk of recurrence depending on the factors involved with the previous birth including gestational age and number of pregnancies (Goldenberg *et al.* 2008), but the exact mechanisms underlying this phenomenon remain unclear. In terms of number of pregnancies, it is speculated that after a pregnancy, the uterus requires time to return to a normal state and resolve any residual inflammation before a second pregnancy. Therefore although it is not understood why, women who have an interpregnancy interval below 6 months have an estimated 2 fold increased risk of preterm birth (Goldenberg *et al.* 2008).

Factors that are currently understood to contribute to the high rate of prematurity in the US have been estimated to account for only one-third of all preterm births, which means that much pertaining to the etiology and pathophysiology of both normal parturition and preterm birth still remains to be explained (Hayes *et al.* 2010) and therefore a more complete understanding is an important aim for biological research. Along with the elucidation of several of the risks for preterm birth, a few of the biological mechanisms behind this disorder have been discovered including; infection, inflammation, uterine overdistension, and stress, all have the ability to activate the normal labor processes of parturition early (Goldenberg *et al.* 2008), but the mechanisms of initiation of these pathways remain unexplained. The identification of such mechanisms will only currently allow proper preparation for premature delivery. This is because currently once initiated this process is irreversible. The most studied and well known cause of preterm birth is the early induction to a normal process of parturition called rupture of the fetal membranes.

1.2 Rupture of the Fetal Membranes

Parturition, or the act of giving birth, normally occurs in humans after a 38-42 week gestation period. During the end of gestation a series of events must occur so that the delivery of the baby proceeds normally. Those events include uterine activation, cervical ripening, and fetal membrane rupture. Among the events of parturition, rupturing of the fetal membranes (ROM) is critical for the correct onset and development of labor (Arikat *et al.* 2006) and for the normal delivery of the baby. The fetal membranes consist of three layers (Figure 2), the amnion, chorion, (fetal) and decidua (maternal), which can collectively be considered as extensions of the placenta that envelope the developing fetus (Hieber *et al.* 1997). During fetal growth, it is vital for these membranes to be strong enough to withstand significant stretching to accommodate the

growing fetus as gestation advances, and also its increased movement (Bryant-Greenwood 1998). This is because it is vital that the fetal membranes encapsulate the baby for its protection, to maintain maternal/fetal communication and to serve as an immunological barrier between the mother and fetus. Thus, it is paramount that rupture of such an essential organ only occurs upon the completion of gestation for delivery of the baby.

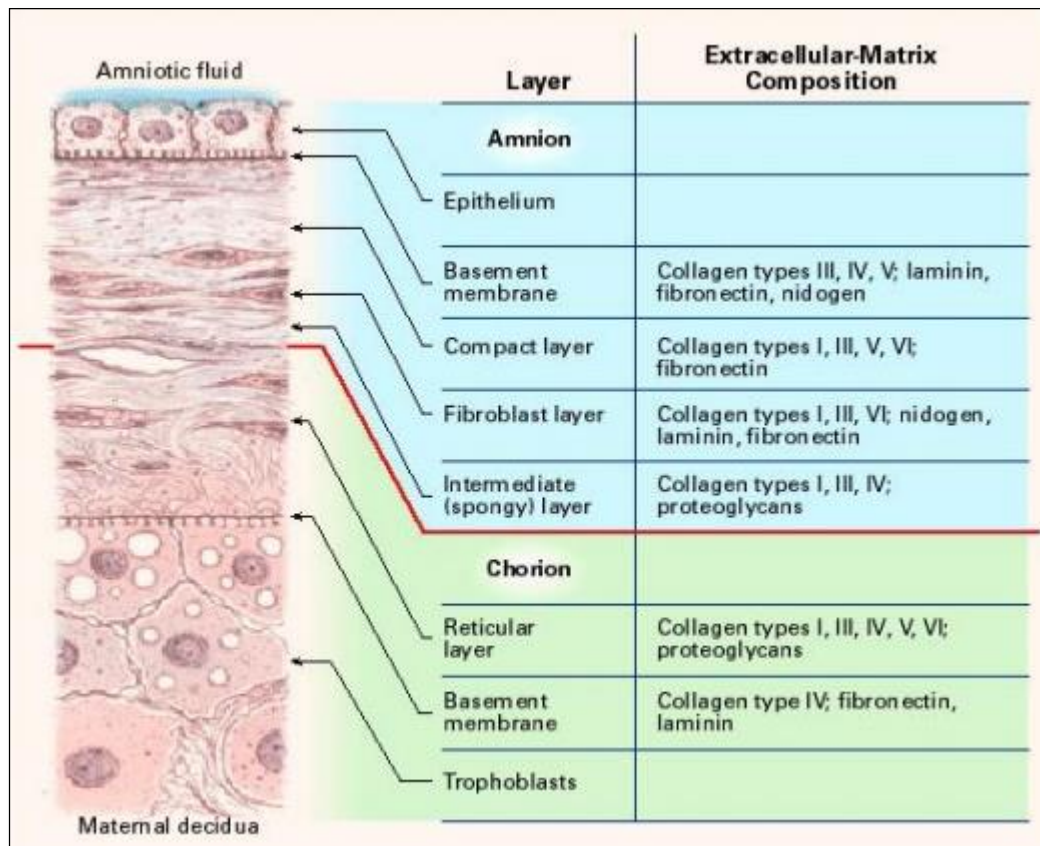


Figure 2. Layers of the human amnion and extracellular matrix components. (Adapted from Niknejad et al. Properties of the Amniotic Membrane for Potential Use in Tissue Engineering. *European Cells and Materials*. 2008)

For membrane rupture to occur normally a specific sequence of events unfold that also involve changes in both the uterus and cervix. Prior to the initiation of normal parturition, the uterus is quiescent due to the inhibition of myometrial activity (Challis 2000). A variety of

myometrial activity inhibitors such as progesterone, prostacyclin (PGI₂), relaxin, parathyroid hormone-related peptide (PTHrP), and nitric oxide (NO), keep the uterus dormant through numerous signaling pathways whose general function is to inhibit the release of Calcium (Ca²⁺) or decrease the enzyme activity of myosin light-chain kinase (MLCK) (Challis 2000). Thus, as smooth muscle contraction is governed by the binding of Ca²⁺ to calmodulin, an inhibition of Ca²⁺ release will prevent uterine contractions and induction of parturition. There is also a concomitant up regulation of contraction-associated proteins (CAPs), like prostaglandins and oxytocin (Challis 2000), causing the uterus to move from a quiescent stage to an activated stage. Upon activation, contractions begin after the conformational change of actin and myosin (Challis 2000).

Cervical ripening also needs to occur during this time causing cervical dilatation in preparation for the transit of the fetus through the vaginal canal. Extracellular matrix (ECM) remodeling of the cervix by MMP-1 and MMP-8, apoptosis, and cytokines causes cervical softening and allow cervical dilation (Ludmir, Sehdev 2000). However, the dilatation of the cervix can also lead to distention of the fetal membranes and the creation of a 'fore-bag' structure. This fore-bag forms in the lowermost portion of the amniotic sac that falls through the cervix and is often where normal membrane rupture occurs. Although not occurring in every pregnancy, the creation of the fore-bag makes it easier for the events related to the rupture of the fetal membranes to transpire. Firstly, the amnion separates from the outermost fetal membrane, the chorion, which then ruptures (Arikat *et al.* 2006). As the amnion is stronger and more ductile than the chorion, after the chorion has ruptured, gravity continues to work on the amnion, significantly distending it with fluid until it ruptures (Arikat *et al.* 2006). The work that demonstrated this sequence of events in membrane rupture clearly revealed that the strength of

the fetal membranes lies within the amnion. There are instances where these membranes do not break and manual rupture is required. If this does occur, there are no detrimental ramifications for the baby; however, it is when these membranes rupture prematurely that concern arises.

Although the influence of gravity on the amnion contributes to its rupture, during normal rupture many biological mechanisms work symbiotically with this force leading to the gradual weakening of the whole fetal membranes. This happens in the form of the remodeling of the ECM and the apoptosis of resident cells, occurring as a result of changes in autocrine/paracrine signaling causing an up regulation of several cytokines. Central to ECM remodeling is the induction of the matrix metalloproteinase (MMP) cascade, initiated by the loss of the interaction of fibronectin with its receptor causing the release of MMP-1 and MMP-3, followed by release of MMP-2 and MMP-9 (Bryant-Greenwood 1998). The MMP cascade is inhibited by tissue inhibitor of metalloproteinases (TIMP) prior to induction and the MMP/TIMP ratio governs matrix remodeling in terms of expression of the MMP cascade. Previous studies have also shown that there is an inverse relationship between the increase of MMP-9 protein and the strength of fetal membranes, as MMPs hydrolyze ECM components (Khwad et al. 2005) directly causing the weakening the fetal membranes. The induction of the MMP cascade along with loss of cell contacts with the ECM in response to stretch, is hypothesized to initiate a resultant apoptosis cascade (Bryant-Greenwood 1998) through induction of caspase 3 and 9 (Reti et al. 2007). Together, these two pathways lead to the degradation of the ECM (Bryant-Greenwood 1998) and generate the weak zone of altered morphology (ZAM), directly above the cervix. In direct support of the role of these cascades in the generation of the ZAM, this area was shown to exhibit an increase in MMP-9 protein (Khwad *et al.* 2005) compared to sites in the fetal membrane away from the cervix.

1.3 Preterm Premature Rupture of the Fetal Membranes

ROM is a process central to parturition, however, it does not always occur in a timely fashion. Therefore, if rupture of this important structure occurs prior to the end of gestation can lead to the premature delivery of the fetus, when fetal development is incomplete. This early delivery can be as a result of fetal distress launched by exposure to infection, inflammation, or insufficient amniotic fluid. Preterm premature rupture (PPROM) of the fetal membranes is defined as fetal membrane rupture occurring prior to the 37 week of gestation with or without labor and is the cause of one third of all preterm deliveries (Mercer 2004). The earlier a baby is born, the more severe their health concerns will be. One consequence associated with preterm birth is delivery before the organ development is complete as seen when babies are born prior to 36 weeks with inadequate lung development (Sadler 2012) at birth, preventing efficient respiration. The most frequent cause of PPRM, causing between 25-40% of cases, is intrauterine infection by a number of organisms such as, *Mycoplasma spp*, *U urealyticum*, and *Streptococcus agalactiae* (Goldenberg *et al.* 2008), ascending from the vaginal cavity. However, the timeframe of the ascent of infection remains unknown, but has been speculated to occur during the second trimester when the membranes are compact against the decidua (Goldenberg *et al.* 2008) allowing the infection to directly contact the fetal membranes and can gain access into the amniotic cavity causing fetal distress. While antibiotics can somewhat halt the spread of infection, the inflammation associated with this infection is not resolved and thus PPRM results. There are currently no treatments for the ‘repair’ of the fetal membranes subsequent to rupture, thus current therapeutic strategies, like daily vaginal progesterone administration or magnesium sulphate for uterine inactivation, attempt to prolong pregnancy to allow more time for fetal development (Werner *et al.* 2011; Crowther *et al.* 2002).

1.4 The Use of Animal Models in Preterm Birth and PPRM Research

Before the consistent high rate of preterm birth in the U.S. and unknown mechanisms of PPRM can be determined, an increased understanding of how normal parturition ensues needs to be realized. Research on parturition, especially in the field of PPRM, is difficult due to the ethical constraints surrounding working with pregnant humans, but also because of the inappropriate nature of many animal models. Certain model animals are adequate for studies dealing with particular aspects of parturition, like some facets of preterm birth caused by infection, and inflammation; however, they are not generalizable for research attempting to elucidate the biological mechanisms behind fetal membrane weakening and membrane rupture. There is considerable difficulty using different animals to study parturition, as there are a number of significant differences in basic anatomy, but also in the physiological mechanisms fundamental to parturition. Most mammals including mice and sheep, initiate parturition upon the elevation of prostaglandins causing a dramatic decrease in the level of circulating progesterone (Roizen *et al.* 2008). This leads to activation of the myometrium and labor contractions. However, in humans, guinea pigs, and nonhuman primates, labor is not governed by a decrease in the circulating level of progesterone, but by a functional down regulation of the effect of progesterone through a change in receptor isoform expression. This receptor change results in a functional progesterone withdrawal causing a decrease in the efficacy of progesterone as a myometrial activity inhibitor (Welsh *et al.* 2014). Therefore, in humans, the change in progesterone receptor is what governs the up regulation of the contraction-associated protein and prostaglandin, moving the uterus from a quiescent stage to activated as part of the mechanism behind the initiation of fetal membrane rupture. This fundamental difference in progesterone control and prostaglandin release negates the value of many model animals (Roizen *et al.* 2008) for ROM research. The reproductive biology of nonhuman primates is the most similar to

humans as far as labor being preceded by a systemic progesterone withdrawal; however, availability and financial cost tends to be a hindrance to their universal use (Institute of Medicine 2007; Elovitz, Mrinalini 2004). More importantly than availability and financial constraints, the constant upright posture of humans forces the fetal membranes to withstand an exorbitant amount of stress from downward gravitational pull compared to nonhuman primates (Figure 3), which renders them a disputable model animal for ROM (Bryant-Greenwood 1998). Therefore, with the numerous differences in hormonal regulation, placentation, gestational length, and fundamental anatomy, there is a real need for most of the mechanisms of ROM to be investigated using human tissue in order to understand the complexity of this human condition.

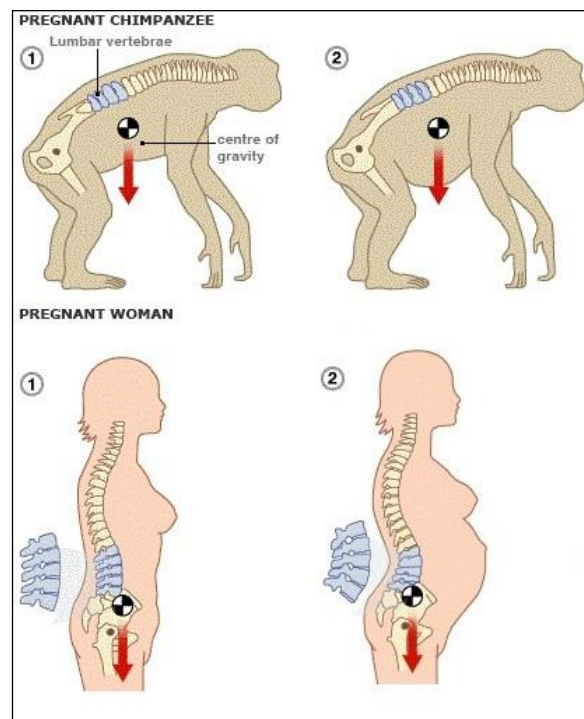


Figure 3. Center of gravity in pregnant chimpanzee and human. (Adapted from BBC News. Curvier spines aid pregnant women. <http://news.bbc.co.uk/2/hi/health/7137104.stm>)

1.5 The Strength of the Fetal Membranes Lies with the Amnion

As previous studies have demonstrated that the strength of the human fetal membranes stems from the amnion, at six times the strength of the chorion, the integrity of the amnion during pregnancy and its timely degeneration are critical to this specific layer of the fetal membranes' function (Arikat *et al.* 2006). Thus, the stronger and more complete the integrity is, the less likely it is that the membrane will rupture.

The human amnion is composed of three layers equaling a sum of 50 μ m in thickness (Chua, Oyen 2009). The innermost apical layer is continuous throughout the amniotic sac and comes in direct contact with the amniotic fluid (Figure 2). It is an epithelial cell monolayer sitting on a collagen IV rich basement membrane (Rampersad *et al.* 2011) and is the source of endogenous prostaglandins for parturition activation (Mortimer *et al.* 1985). Below is the mesenchymal layer, which is rich in various collagens and elastins, secreted by the mesenchymal cells (AMC) providing its strength and impressive elastic characteristics respectively (Chua, Oyen 2009) (Figure 2). The third layer of the amnion is below this durable layer and is composed of a spongy ECM rich layer that has evolved to provide cushion to the previous layers, especially in early development when the amnion can slide over the chorion allowing for the fusion of the two membranes (Bryant-Greenwood 1998) (Figure 2). The intermediate spongy layer is also able to absorb water and by doing so, the amount of stress on the fetal membranes can be buffered. However, as this layer takes on more water towards the end of gestation it pushes the collagen fibers apart and this can weaken this layer (Bryant-Greenwood 1998). The remodeling of the mesenchymal layer's ECM via autocrine/paracrine signaling, occurs during the normal weakening process before membrane rupture, but also needs to happen in some form for PPRM

to occur (Bryant-Greenwood 1998). This remodeling occurs when the resident cells go through apoptosis as in their absence the ECM components, mainly collagen, cannot be replenished.

1.6 Collagens of the Mesenchymal Layer and the Amnion Mesenchymal Cells

Studying the amnion mesenchymal layer is of central importance to understanding normal membrane rupture as it is thought to be the cornerstone of amnion strength due to its high composition of various forms of the protein collagen. It consists mostly of fibrillar collagens type I and III with smaller amounts of V and VI (Bryant-Greenwood 1998) which work together to form collagen fibrils. These fibrils are fortified by covalent cross-linking of their lysine residues, that when prohibited, decrease tensile strength and the tissue becomes fragile (Alberts et al. 2008). Since the strength of the fetal membranes is due to the various collagens present in the amnion, understanding the resident cells that synthesize and control their turnover is vital to unlocking the mechanisms of ROM. Studies have demonstrated that the cells of the mesenchymal layer are primarily, if not exclusively, responsible for the synthesis of the interstitial collagens, as a decrease in the synthesis of collagen by AMC correlates with the timing of gestation; the closer the cells are to the end of gestation, the less collagen they form (Casey, MacDonald 1996). This decrease in collagen synthesis is paralleled by a decline in numbers of AMC during this time. (Casey, MacDonald 1996) Indeed, this work strongly support the current dogma in the field that the strength of the amnion stems from the collagens generated by the AMC.

To understand the mechanisms behind the amnion and membrane rupture, a core characteristic belonging to AMC needs to be considered. This is that these cells are often highly desired in various fields of study from cell therapy to tissue regeneration and other potential stem cell applications as they have the ability to differentiate into mesoderm, ectodermal, and

endodermal cell types (Parolini *et al.* 2008). Thus, due to this pluripotent ability, AMC in culture are predisposed to differentiate into multiple cell lineages not typical to their *in vivo* state in the human amnion. After isolation, AMC can be cultured on plastic dishes where they adhere, proliferate, and withstand several passages, but proliferation slows beyond the second passage (Parolini *et al.* 2008). Therefore, the careful characterization of these cells is essential to understand their normal physiological role in the amnion, as these primary cells are able to change phenotype while *in vitro* (König *et al.* 2014). AMC normally exhibit a polar-free fibroblast morphology *in vivo* that changes into a flattened hypertrophic monolayer *in vitro*. In order to generate a system for *ex vivo* study of ROM and minimize the caveats associated with the data generated, it seems reasonable to suggest that AMC need to be studied in a system that is most similar to their *in vivo* conditions.

1.7 2D Cell Culture

While *in vivo*, AMC are dispersed and embedded within the middle collagen rich layer in the amnion where they are free of cell polarity. However, to date they have almost exclusively been studied in a classic 2D cell culture system, which is therefore not typical of their *in vivo* environment (Bryant-Greenwood 1998). 2D culture has afforded advances in numerous concepts including the generation of immortal cell lines, vaccine formation, mechanisms of virology (Drummond *et al.* 1997; Henderson, Galloway 1953; Belser *et al.* 2013) and cell identification. Therefore, they have been extremely valuable as a simple way to understand convoluted mechanism. Established in 1907, 2D culture rapidly became a foundation technique of cell and molecular biology, as biologists can easily grow, observe and manipulate cells (Shamir, Ewald 2014). However, it is now thought that these methods may not be best suited for all cells, especially those like AMC or those that rely on interaction with other cell types for their

‘true’ physiological responses. Using AMC as an example, when they are grown on a plastic tissue culture dish, they rapidly reflect an apical-basal polarity (Figure 4), which is not one of their natural characteristics (Shamir, Ewald 2014). This leads to changes in morphology, as their appearance becomes flattened and spread, presumably due to the lack of an extracellular matrix contacts all around the cell which is already known to govern cell viability and function. Indeed, their apparent distress at their new environment is easily illustrated by the rapid production of stress fibers. Thus, it seems that these cells need to make multiple cell adhesions three-dimensionally to maintain their *in vivo* morphological characteristics and presumably their authentic biological response. Evidence to support this comes from work that illustrates that cell morphology is dictated by the cell-matrix interactions, organized with the help of integrins, fibronectin, paxillin, and other adhesion molecules, that mediate several pathways including proliferation, differentiation, migration, cell survival, tissue organization, and remodeling of the matrix *in vivo* (Cukierman *et al.* 2002; Baker, Chen 2012).

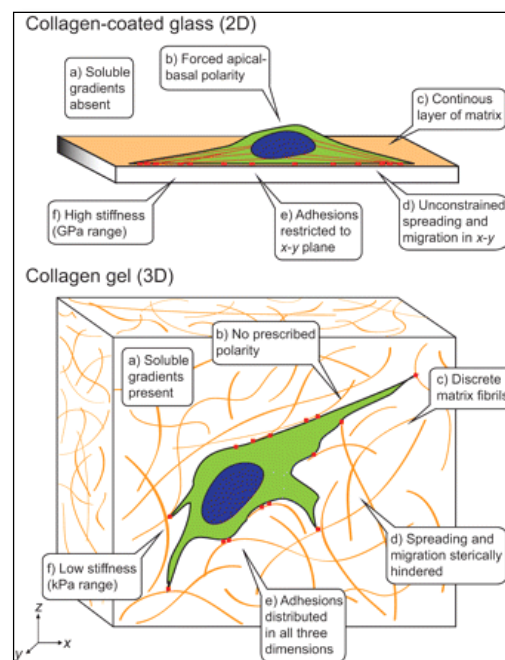


Figure 4. Polarity of cells in 2D and 3D culture. (Adapted from Baker, Chen Deconstructing the third dimension- how 3D culture microenvironments alter cellular cues. 2012)

It has also been shown that in 2D culture, due to the lack of cell-matrix interaction other than at the basal surface, gene expression can be altered (Knight, Przyborski 2014) compared to 3D counterparts. Studies that have utilized mouse mesenchymal cells show a difference in focal and fibrillar cell-substrate adhesions *in vitro* compared to those seen a 3D *in vivo* representation (Cukierman *et al.* 2001). While using the mouse cell model, researchers visualized a colocalization of focal and fibrillar adhesions by labeling paxillin and $\alpha 5$ integrin respectively in 3D, which is not seen in 2D (Cukierman *et al.* 2001). Interestingly, these *in vivo* adhesions were parallel to extracellular fibers containing fibronectin (Cukierman *et al.* 2001), a key glycoprotein in cell-matrix interactions. To fully grasp concepts of AMC and understand their function, potential differences in the traditional 2D culture could alter the interpretation of AMC *in vivo*. Therefore, a different culture method with the ability to place AMC into a similar environment to *in vivo* needs to be established.

1.8 3D Cell Culture

Novel 3D cell culture techniques were established to address some of the issues seen with some cells in 2D culture, to enable investigators to study more complex multicellular systems and to more closely mimic *in vivo* environments. Many different approaches to building novel 3D culture techniques have been established and include; embedded cultures, matrigels, co-cultures, and mechanically supported membranes. All of the methods have attempted to minimize cellular aberrations in behavior and physiology by more accurately duplicating *in vivo* environments (Shamir, Ewald 2014). The experiments that have utilized embedded organoids into ECM gels have made significant breakthroughs to several unknown concepts such as the branching morphogenesis of mammary glands, kidney, and lung that were previously unattainable in 2D culture (Ewald *et al.* 2008; Qiao *et al.* 1999; Liu *et al.* 2004). Advances in

biological mechanism have also been established using mechanically supported culture inserts where epidermal keratinocytes were seeded to form an initial monolayer (Shamir, Ewald 2014). Over time these cells stratified and differentiated into an epidermis-like structure once exposed to an air-liquid interface allowing sophisticated studies of disease and development of the integument (Shamir, Ewald 2014). Another innovative 3D culture method of cellular aggregate culture creates a hanging media drop technique that forms spheroids that is now often the preferred way for cancer research to create a mixed population of proliferating and quiescent cells based on their location within spheroids (Mehta et al. 2012). These aggregate cultures can also be used in drug resistance and sensitivity studies that may yield conflicting results compared to 2D culture models, as studies show clear differences in energy metabolism between the two culture methods (Santini *et al.* 2003). Thus, the pharmaceutical industry is rapidly switching to 3D tissue culture methods as a way to glean more accurate physiological and pharmacological data as 3D aggregates show an increase in resistance to chemotherapy and radiotherapy compared to their 2D counterparts (Knight, Przyborski 2014).

As well as the biological mechanistic improvements seen by switching to 3D culture techniques, the increased use of more comprehensive culture methods reduces the number of animals sacrificed for research and can lead to significant financial gains. In addition, more complex culture models present a faster way to study mechanisms on a tissue level with improved control over experimental parameters.

1.9 Study Purpose

With novel 3D culture approaches leading to the discovery of previously unknown concepts, it is easy to speculate that 3D culture can unmask some of the possible mechanisms underpinning preterm birth, the cause of membrane rupture initiation, and to also allow the

testing of pharmacological treatments for the amnion pertaining to ROM and PPROM. Preterm birth remains a significant problem, and current methods of research have not as yet yielded solution, a more complex culture system approach is needed to understand the local mechanisms that rule fetal membrane rupture in order to elucidate which may be altered in preterm birth. Given that exciting new breakthroughs have been exposed once researchers have switched cells from studying cells in a 2D environment to a 3D environment, it seems that novel substantial breakthroughs could occur if a similar approach was taken to the study of AMC. This could lead to a closer comprehension of *in vivo* cellular organization and function. Therefore, the purpose of this work was **to generate a novel 3D culture system for human amnion mesenchymal cells and evaluate its potential to study the amnion by (1) the characterization of AMC survival and morphology and (2) describe the gene expression profile of the cells grown in the 3D model compared to a traditional 2D system.** It is thought that this will circumvent the issues of missing cell-matrix interactions of AMC in 2D culture that mediate several pathways of cell viability, metabolism, and function.

By establishing a novel 3D culture system for AMC, it is hoped that this model be used to extend the understanding of the human amnion and research the mechanisms of PPROM. Thus, the goal of growing AMC in an environment closer to *in vivo* could allow AMC to revert back to a physiological state similar to their origin.

2.1 Introduction

Historically, the use of a 2D culture system rapidly increased our ability to learn many of the intricacies of biological mechanisms that were previously impossible to discover using the biological methodologies available at the time. However, several limitations remain if taking approach, as cells grown in this manner are limited to an isolated cell population, lack extracellular matrix attachments three dimensionally, and often sit in a stagnant supply of nutrients. Three-dimensional cell culture techniques have been developed in an attempt to improve the accuracy of the replication *in vivo* environments. These novel models have enabled researchers to study increasingly complex systems, which have already garnered advances in various fields including branching morphogenesis of the kidney. In this instance, before 3D technologies were implemented, the dogma was that branching morphogenesis was induced by direct contact of the epithelial cells of the ureteric bud with the mesenchyme. However, when researchers isolated rat ureteric buds and placed them into a 3D ECM gel, they noted that branching morphogenesis was not dependent on the mesenchyme and that the ureteric bud could undergo this process alone *ex vivo* (Qiao et al. 1999) and thus thinking in this field was transformed. As has been demonstrated in several other areas of biomedical research, the power of 3D models to transform what is known about biological mechanism may also be true if this approach was applied to the study of AMC for ROM research. This is because many key aspects remain unknown about the role of these cells in the rupture of this tissue. This field of biomedical research is stagnating due to the very real limitations of this research; there is a lack of appropriate animal models and human focused work relies on freshly collected term tissues within which the primary cells predisposed to apoptosis and are embedded in a rapidly degrading

ECM. A 3D model could circumvent some of these lingering issues allowing researchers to rebuild the amnion of the fetal membranes allowing the cells to adapt to and interact with ECM and take on a morphology that is similar to their original *in vivo* state.

3D cell culture models are currently not used for ROM research. Indeed, only a few studies have made attempts to develop a 3D culture system for AMC, however, those studies were not focused on ROM, but aimed to use AMC in tissue engineering applications, due to their pluripotent capability and high immunological tolerance for transplantation (Mihu et al. 2009). Therefore to date, the most informative attempt to study AMC in 3D was one designed as a model for the engineering fetal membrane patches to repair early rupture (Bilic *et al.* 2005). This model demonstrated that while in a collagen I or fibrin matrix, AMC can migrate and acquire an *in vivo* phenotype with long cellular extensions. This showed that AMC not only have the capacity to retain their ability to adapt to their environment after removal from the fetal membranes, but also demonstrated that this kind of 3D culture approach could prove valuable for ROM research. Thus, it is thought that the use of a 3D model for AMC culture has the potential to radically improve our understanding of the mechanisms of fetal membrane rupture, as these cells would be expected to behave more similarly to how they do *in vivo* at the end of gestation. This could, therefore, ultimately translate into new potential therapies for PPRM and thus go some way to provide some relief to the high preterm birth rate in the United States that is currently unobtainable with current approaches.

The original concept of studying cells removed from organs in culture was not designed to study convoluted biological mechanisms, but as a way to study individual cell biological change over time. This was in stark contrast to the end point or ‘snap-shot’ data that could have been gleaned from chemical measurement, histological or anatomical analysis. Thus, a 2D study

approach, while a large leap forward, still often limits research to a strictly homogeneous population of cells with a stagnant nutrient supply, which can also simulate a different environment compared to that experienced inside the body. While *in vivo*, cells function as heterogeneous units relaying signals from one cell to another and one organ system to another, with a constant flow of nutrients supplied by blood vessels. Thus, the cells of the body work together to maintain a state of homeostasis, however much of this important functional communication is lost in 2D culture. In addition, for a variety of cell types, 2D culture forces cells into an even more abnormal environment; for example, lung cells that become flooded with a liquid or cardiomyocytes that are designed to constantly be in motion, both of which are lost in 2D culture. The ECM is another vital part of organ structure that is largely missing in 2D culture, these secreted proteins are what give tissues their structure and strength, and also enable cells to interpret and translate physical changes in the environment.

As with the development of all novel models, care needs to be taken to validate new methodological approaches. Thus, advances in the development of new 3D cultures need to be characterized so that the results are not subject to unnecessary caveats, perhaps invalidating the model entirely. Therefore, when a new 3D system is generated it is necessary that the preservation of the integrity and behavior of cells are demonstrated, otherwise the model may become invalid for downstream biological application. One approach to validate a new model that has been commonly practiced for 3D culture validation, is to establish a pure cell population (Rodriguez-Fuentes *et al.* 2015; Sharma *et al.* 2013), identify cell adherence properties (Rodriguez-Fuentes *et al.* 2015), proliferation and migration ability (Reinnervate 2014; Sharma *et al.* 2013; Bilic *et al.* 2005), cellular morphology (Reinnervate 2014; Santini *et al.* 2003; Vergani *et al.* 2003), and study their function, such as pluripotency (Reinnervate 2014). All of

these measures aim to ensure the model produces study results are a true representation of cellular function. Cell viability has been a large concern in 3D culture development due to the variety of 3D methods and location of cells within these constructs. The often-used 3D spheroids are ideal for cancer research as they have the ability to establish mixed cell populations. However, the cells in the center of the spheres are prone to apoptosis and necrosis, as they do not come into direct contact with nutrients (Mehta *et al.* 2012). Therefore, while 3D culture methods can be powerful, each model can come with specific stipulations that must be considered when interpreting the data generated. Advantageously, the amnion is an avascular structure and therefore this negates some of the concern regarding the appropriate acquisition of nutrients in culture. *In vivo*, this layer of the fetal membranes acquires its nutrients through the closest blood vessels of the underlying chorion. Even though the acquisition of nutrients in 3D models of the amnion is of minimal concern, there are several other validation aspects; of cell contamination, adherence, proliferation, and migration that warrant consideration.

Previous data generated in the Wright lab (unpublished data) culturing AMC in 3D as a technique for fetal membrane research, showed that both matrigel and egg white albumin lead to drastic changes in cellular morphology. The cells were seen to transition from a typical fibroblast appearance, forming spherical clusters of cell bodies with complex networks of processes that somewhat morphologically resembled neurospheres. Even though these studies clearly demonstrated that AMC have the capacity to adapt to environmental cues and they have the potential for trans-differentiation, the abnormal morphology observed made these two approaches inappropriate as models to specifically understand the amnion and the mechanisms of ROM. This also demonstrated the need for a more considered approach to the generation of a

new 3D system to understand the mechanisms of interaction of the endogenous cells of the amnion with their ECM that lead to ROM.

A leading 3D cell culture development company, Reinnervate, have developed a scaffold (Alvetex) composed of an inert polystyrene material that eliminates the use of foreign animal proteins for routine 3D cell culture. A key concept behind their product is that it is extremely porous, attempting to aid in the availability of 3D attachments for cells with the hope that they will then mimic their *in vivo* morphology and function (Knight et al. 2011). The beauty of this porosity is that it also allows nutrients and other solutes to move freely throughout the culture system (Knight et al. 2011). Studies have documented that cells are viable in this polystyrene scaffold as Alvetex scaffolds have been populated with many different cell types, including primary mesenchymal cells from rats. The rat cell proliferation rate was seen to increase over a 14 day period, with cellular population throughout the scaffold (Reinnervate 2015). In addition, using the same approach the culture of the MG63 osteosarcoma cell line also resulted in robust cell proliferation and migration of these cells throughout the entire scaffold, with an increased complexity of morphology compared to 2D culture (Reinnervate 2015). This work also nicely demonstrated that the polystyrene scaffold allows multiple cell-matrix connections. Thus, the prospect of using this polystyrene has potential for adaptation to an AMC model, with its porosity allowing a constant flow of nutrients, availability of cell attachments, and improved function demonstrated by other mesenchymal cells. The artificial ECM scaffolding of this 3D system, which in this instance is an inert polystyrene honeycomb, should allow AMC to retain their fibroblast shape due to the increased availability for cell attachment without the added complication of ensuring the ‘perfect’ ECM protein combination to provide the specific signals for this cell type.

Therefore, the hypothesis for Aim 1 of this thesis was that culturing AMC in the Alvetex scaffold would enable the growth of viable cells that more closely morphologically mimic those from an *in vivo* environment when compared to 2D culture methods. It was expected that the porous scaffold would allow the AMC to retain non-polar characteristics and thus keep their normal fibroblast morphology as opposed to the flattened appearance they characteristically exhibit in 2D. In order to test the hypothesis for this aim, three sub aims were designed to characterize the novel culture system based on establishing appropriate seeding density, determine how the cells proliferated over time, their morphology, and their survival traits.

2.2 Aim 1: To perform a Characterization of a novel AMC 3D Culture System to improve the understanding of the role of these cells in the amnion and ROM

*Aim 1a: To generate a novel 3D culture system for AMC that is comparable to the *in vivo* based on a pure AMC population, cellular density, and morphology.*

Rationale: A seeding density that is comparable to that seen *in vivo* needed to be established first to minimize the potential for abnormal morphology, which may also effect cell survival characteristics. This is because it has already been shown that AMC are highly adaptive to their environment by their behavior in previous 3D cultures (Rodriques-Fuentes *et al.* 2015; Bilic *et al.* 2005). Environmental cues dictating morphology and survival can include growth media, but also the proximity of one cell to another, making initial seeding densities of cells important to determine how these cells will behave in culture due to the known correlation with cell viability. For example, seeding cells at high densities can inhibit proliferation and seeding them too sparsely can decrease cell survival, which are a result of the availability of nutrients in the culture system and the ability of cells to interact and signal with each other. Thus, there is an inverse relationship between cell proliferation and seeding density as if cells are seeded too

dense, there is a decrease in nutrients available for each cell (Pledimonte *et al.* 1982). Therefore, when generating a novel 3D system, it was vital to find a good balance of seeding density as it can affect the outcome of cell survival while still maintaining an environment similar to *in vivo*.

During isolation, AMC are collected by a collagenase I treatment upon the completion of several serial trypsin digestions. However, despite the final washing techniques once AMC are plated, there may still be contamination in the cell cultures due to residual amnion epithelial cells (AEC), which are not the cells of focus for this study. Even more concerning is that their presence could alter AMC expression patterns in downstream experiments, either due to cell type interaction or by them exhibiting a differential expression pattern to AMC that would then be experimentally combined upon data collection. The isolation method used has been shown in previous studies to yield about a 98% purity of AMC upon initial seeding (Casey, MacDonald 1996) making the likelihood of AEC contamination in a passage 4 AMC culture minimal, but still considered important to confirm.

Aim 1b: To determine the effect of time on AMC density in culture

Rationale: In order for the continuation of downstream experiments for cell survival and gene expression, a density and migration evaluation of AMC was determined over time in the novel 3D culture system. AMC require time to re-adhere since contact with trypsin during each cell passage strips their surfaces and forces them to retract their adhesions that need to be re-modeled for new attachments. In addition, if these cells remain in culture too long, they can stop proliferating and become apoptotic, as these cells are predisposed to cell death upon the completion of gestation alongside the loss of ECM contacts during normal weakening of the fetal membranes (Bryant-Greenwood 1998). However, a short period in culture could result in the

cells not having enough time to migrate within the scaffold and proliferate. This too, will alter cellular responses in downstream experiments and perhaps not give a true representation of AMC *in vivo* characteristics. Therefore, AMC cultured for an inadequate amount of time may become inappropriate for further use to study. Seeding AMC too densely will also create an environment not typical of them *in vivo*, as these cells are relatively sparsely found within their collagen matrix. Since the goal is to create an environment comparable to *in vivo*, a high seeding density will also not realistically mimic AMC in the amnion.

Aim 1c: To measure the Cell Survival Characteristics of AMC in 3D culture and compare them to 2D culture

Rationale: To ensure the novel AMC culture method can be utilized for future studies, the cell survival characteristics of cells resident in this model were determined. Apoptosis, necrosis, cytotoxicity, and hypoxia are factors that are important to be taken into consideration during the culture of cells not only because they alter the cell survival rate that could lead to cellular demise, but also because they have the potential to alter cellular behavior. Particularly, apoptosis is important to evaluate, as AMC collected for this thesis were isolated from term amnion making them especially vulnerable to apoptosis as many have already begun the process *in vivo*. Cells grown in culture also have the potential to undergo secondary necrosis, or passive cell death, as *in vitro* apoptosis occurs (Elmore 2007). Necrosis is the result of cell injury that promotes cascades affecting cell viability such as tumor necrosis factor (TNF), reactive oxygen species (ROS), and Fas-associated protein with death domain (FADD) signaling (Golstein, Kroemer 2006). These cell death pathways could alter cellular cues for downstream experiments preventing the measurement of *in vivo* AMC behavior. The level of hypoxia is also an important parameter to measure as it can compromise cell growth and viability. Induced in the absence of

oxygen, hypoxia usually leads to the upregulation of angiogenesis pathways in an attempt to create an oxygen supply to tissues. The absolute amount of hypoxia that the cells are subject to *in vivo* is uncertain, as the amnion is an avascular tissue. However, it is known that in 2D culture AMC can be induced into an endothelial lineage if left in a hypoxic environment (Maruyama *et al.* 2013). A hypoxic environment causes release of the transcription factor, hypoxia inducible factor 1-alpha (HIF-1 α) in an attempt to aid the cells' return to homeostasis controlling migration, metabolism, and cell survival. Thus, the levels of apoptosis, necrosis, proliferation and hypoxia are all pathways that can interfere with cellular behavior and control cell viability, which could render the novel culture system invalid for use to study the amnion, ROM, and PPROM.

2.3 Materials and Methods

Cell Isolation: Human fetal membranes were collected from repeat Caesarean section from Kapiolani Women and Children's Hospital with approval by the hospital IRB and UH IRB as an exempt protocol. All parties involved with human tissue collections were ethically trained and aware of IRB regulations and standards. After a small membrane sample was taken and placed in formalin for downstream histological analysis, the amnion was separated from the chorion and washed by placing in 1x PBS with residual blood clots removed by glass slide manipulation. The tissue was minced with scalpel blades and placed in 125mL of 0.2% trypsin (Life Technologies, Carlsbad, CA) diluted in DMEM/F12 (Life Technologies, Carlsbad, CA) media. The amnion then went through a trypsin incubation period for 30 minutes at 130 rpm in 37°C. Between each digestion, the amnion was poured into a sieve and the filtrate discarded. The collected tissue fragments were minced again and placed in another 125mL of 0.2% trypsin. A 3.3mg/mL

Collagenase I (Roche Diagnostics, Indianapolis, IN) solution was prepared by reconstitution into 33mL of DMEM/F12 complete (10%FBS and 5% Pen/Strep) media. 1mg/mL DNase I (Roche Diagnostics, Indianapolis, IN) was also reconstituted into 100mL of DMEM/F12 complete media. These solutions were mixed together and added to the remaining amnion tissue and incubated at 37°C for 1 hour at 150rpm. The cells were gathered by centrifugation at 3,000rpm for 5 minutes where supernatant was discarded. The pellet (average 43,000,000 cells), was suspended in DMEM/F12 complete media and cultured on ten 6cm 2D culture dishes at 37°C and 5% CO₂. After 2 hours, cells were washed with 1x PBS to eliminate any non-adherent cells and new DMEM/F12 with 10% FBS media added. Cells were grown for an average of 1 week, with a media change every 3 days, to about 80% confluency and then each 6cm dish was passed onto 10cm 2D culture dishes. This step was repeated until the total amount of cells was adequate for experiments, (usually between passage 3 and passage 5), which averages 1 million cells per 10cm dish.

Determination of Cell Density: Alvetex scaffolds (Reinnervate, Durham, UK) were primed with Poly-L Lysine (Sigma-Aldrich, St. Louis, MO) by submerging into 70% EtOH for 5 minutes, washing twice with DMEM/F12 complete media, and coated with 1mL of Poly-L Lysine overnight at 4°C. AMC were seeded onto the center of scaffolds at densities of; 50, 100, 200, 300, 400, and 500 thousand per disc in 50µL of DMEM/F12 complete media. Cells were allowed 2 hours to adhere to the scaffolds before the wells were flooded with 5mLs of DMEM/F12 complete media. After 24 hours, the cells were washed 3 times with 1x PBS then fixed with 5mLs of 4% paraformaldehyde (PFA) at 4°C for 18-23 hours. Each disc was then placed serially in 30%, 50%, 70%, 80%, and 90% EtOH solutions for 15 minutes. Before embedding, scaffolds were cut in half and placed in a plastic cassette and then placed in 100%

EtOH for 30 minutes, Histochoice (Sigma-Aldrich, St. Louis, MO) for 30 minutes, and then a 50:50 Histochoice/Paraffin solution for 30 minutes. Then samples were placed in paraffin for 1 hour and embedded (JABSOM histology core). Hematoxylin and eosin stain was performed on a representative section from each scaffold and compared to a fetal membrane roll. Gill 2 Hematoxylin was incubated on scaffolds for 1 minute, washed with distilled water and Eosin added for 30 seconds. Sections were then washed in 0.1% acetic acid water for 30 seconds and dehydrated in EtOH as used initially. Mounting was done with DPX mount (Sigma-Aldrich, St. Louis MO). AMC in the fetal membrane rolls (n=6) and AMC from scaffold histology were tallied with amount of cells per area determined. Length and width of the membrane sections were measured in μm and the density calculated in cells per μm^2 .

Morphology: AMC (n=4) were cultured on Poly-L-lysine primed Alvetex scaffolds and 2D chamber slides at a ratio according to surface area of 219cm² and 1.8cm² respectively of 400,000 and 3,300. After 48 hours in culture, cells were fixed in 4% PFA as before. Samples were permeabilized with 0.1% TritonX-100 in D-PBS (1x PBS containing 0.9mM CaCl₂ and 0.49mM MgCl₂-6H₂O) for 15 minutes and then 5mLs of blocking buffer (800 μL normal goat serum, 80 μL Tween-20 0.1%, and 80mL DPBS) added to samples for 30 minutes. After blocking, 400 μL of Phalloidin (Life Technologies, Carlsbad CA)/DAPI (Calbiochem, Billerica MA) solution (1mL blocking buffer, 1 μL DAPI, and 1.6 μL) was added and incubated for 1 hour in the dark. Upon completion, samples were washed 5 times with blocking buffer for 10 minutes at 45rpm and then mounted with TRIS buffer. Cells embedded in scaffold and on 2D chamber slides were imaged with Epifluorescence and Confocal microscopy (Nikon Eclipse Ti, Nikon, Melville, NY). Imaged were taken using a 20x objective and TxRed filter for Phalloidin and DAPI blue filter for nuclear fluorescence.

Determination of AEC contamination rate by immunocytochemistry: AMC were seeded at 400,000 per scaffold and cultured in DMEM/F12 complete media with duration of 2 days, upon which, scaffolds were fixed with 4% PFA as before. AMC within scaffolds were then treated with a 1% Triton X-100 permeabilization solution for 15 minutes then washed with 1x PBS and blocking buffer (5% normal goat serum, 1% bovine serum albumin, and 0.2% triton X-100 in 1x PBS) for 15 minutes. The vimentin antibody (0.153mg/mL) was used at 1/50 dilution in blocking buffer. A no antibody negative control was utilized and this primary antibody incubation step was for 1 hour at room temperature. Scaffolds were then washed with 1x PBS then secondary antibody, Alexa Fluor 488 goat anti-rabbit (Life Technologies, Carlsbad, CA) was added and incubated for 2 hours at room temperature in the dark. After the secondary antibody incubation, samples were incubated with a 1uL/5mL DAPI solution for 1 minute at room temperature and washed 3 times with 1x PBS. Whole scaffolds were mounted onto slides using TRIS buffer and imaged with Epifluorescence microscopy (Nikon Eclipse Ti, Nikon, Melville, NY) where cells were quantified by counting cells expressing vimentin and those only identified by DAPI label. Quantification was performed using a stereology method that utilizes a disector principle to avoid double counting of cells unbiasedly in a 2D volume. A preliminary count was performed by moving the counting fields from top to bottom of the disc for three complete passes of the scaffold, at a magnification of x60. AEC percentage was then calculated to give a percent contamination rate.

Cell Density over Time: AMC (n=3) were seeded at a density of 400,000 and 500,000 (n=2) onto Alvetex scaffolds treated with Poly-L Lysine for up to 7 days. Cells were cultured as before. Media was replaced every other day to insure the growing cells had an adequate nutrient supply. One scaffold was selected each day and its cells were fixed (every 24 hours) with 4% PFA at 4°C

and media collected. After 18-24 hours of fixation, the scaffolds were dehydrated in an EtOH series and embedded in paraffin (as per Aim 1a) and H&E stained.

Cellular Proliferation Mitochondrial dehydrogenase activity (MTT) Assay: AMC were cultured at 400,000 cells per scaffold onto seven 3D scaffolds and a density of 600 per well into a 96 well plate. The cells were washed in 1x PBS, with scaffolds removed from their holder, and then placed into a 6-well plate. A negative control well contained a scaffold and a 96 well without cells, but with all of the reagents added. 1mL of 1mg/mL MTT reagent (Millipore, Temecula CA) reconstituted in PBS was added to each scaffold well and 10 μ L to the 96 well plates then incubated at 37°C in 5% CO₂ for 4 hours. Acidified isopropanol solution was generated by mixing 2mLs isopropanol with 2 μ L of HCl and 1mL of this solution was added to each well and placed on a rotating platform for 10 minutes at 100rpm at room temperature. The 96-well plate had the addition of 100 μ L isopropanol with 0.04N HCL added to each well. 20 μ L of the solution from the scaffold wells was added to a 96-well plate with 180 μ L isopropanol creating a 1:10 dilution. The absorbance was read on both 96-well plates at 570nm on a microplate spectrophotometer (Bio-Rad xMark, MPM 6 Alias, Hercules, CA).

Western Blot: Protein was collected from AMC grown in 10cm culture dishes and 3D scaffolds by the addition of 1mL RIPA (radioimmunoprecipitation assay) buffer (50mM Tris, pH 7.4, 1% NP-40, 0.2% Sodium deoxycholate, 150mM NaCl, 1mM EGTA, 0.4M EGTA, ¼ of a protease inhibitor cocktail tablet (Roche, Basel Switzerland), 1mM Na₃VO₄, 1mM NaF) on ice. The 2D cells were removed from their dish with a cell scraper and 1/2mL of RIPA buffer. The 3D scaffolds remained on ice over a period of 30 minutes while being vortexed for 10 seconds every 5 minutes. Lysates were clarified by centrifugation at 15,000rpm for 3 minutes and supernatant

collected. All protein concentrations were determined by a bicinchoninic acid assay (BCA) utilizing the Pierce BCA Protein Assay Kit (Thermo Scientific, Rockford IL).

Protein from the cell lysates were separated according to size in a 10% SDS gel by electrophoresis at 100V for 20 minutes then 200V for 2 hours at -80°C. Upon the completion of separation, proteins were transferred to a nitrocellulose membrane and blocked overnight in 5% milk in 1x PBS-T (1L 1x PBS, 1mL Tween 20 (Sigma-Aldrich, St. Louis, MO)). Primary antibodies were prepared in the 5% milk blocking-buffer. Caspase 3 (R&D Systems, Minneapolis MN), cytochrome c (R&D Systems, Minneapolis MN), and HiF-1 α (Santa Cruz Biotechnology, Dallas TX) were used at concentrations 5 μ g/mL, 0.5 μ g/mL, and 1 μ g/mL respectively. Primary antibody incubation with the membrane was for 2 hours at room temperature. Membranes were then washed three times in PBS-T for 20 minutes. The secondary antibodies of Goat IgG Horseradish Peroxidase (R&D Systems, Minneapolis MN) for caspase 3 and Mouse IgG Horseradish Peroxidase (R&D Systems, Minneapolis MN) and for cytochrome c and HiF-1 α were used at a 1:3000 dilution and incubated on the membranes for 1 hour at room temperature at 40rpm then washed again in PBS-T. An enhanced chemiluminescence (ECL) kit (GE Healthcare, UK) was used according to the manufacturer's instructions, to detect bands by incubation in the dark for 5 minutes. Membranes were then exposed to film using a cassette developer where bands were detected. To ensure even protein loading, the membrane was cut before primary antibody incubation for the proteins of interest and the bottom half probed with a beta-actin antibody (Abcam, MA) conjugated to its secondary antibody (1:300,000) for one hour at room temperature, before detection with ECL. All resultant bands were then analyzed by Image J to determine their relative density.

Lactate dehydrogenase (LDH) assay: Media was collected daily from the time course experiments with matching 2D patient counterparts and stored at -80°C ($n=4$ patient samples) until use. $90\mu\text{L}$ of Tris-HCl (0.2M , $\text{pH } 7.3$), $3.3\mu\text{L}$ NADH (6.6mM), and $3.3\mu\text{L}$ of sodium pyruvate (30mM) were added to a 96-well plate and incubated for 5 minutes at 25°C . $3.3\mu\text{L}$ of each daily media collection was then added to the 96-well plate and the absorbance was monitored at 340nm every 10 seconds over 10 minutes.

Propidium iodide (PI) necrosis assay: AMC were seeded onto a two 3D scaffolds at a density of 500,000 cells and 2D chamber slide density of 4,125 grown for 7 days. One scaffold and slide combination was prepared as a time course day 1 representation and the other set remained in culture for the complete 7 days. Samples were then washed in 2x saline sodium citrate (SSC) $\text{pH } 7.0$. A 500nM PI solution in 2x SSC was generated by diluting the 1mg/mL (1.5mM) stock propidium iodide (PI) 1:3000. $300\mu\text{L}$ of PI solution was added to the samples and incubated at room temperature for 5 minutes. One half of each scaffold and 2D well was sacrificed as a positive control by inducing cell injury with 4% PFA for 20 minutes prior to the addition of PI. DAPI solution was added to samples at a $1\mu\text{L}/5\text{mL}$ dilution for 1 minute. Scaffolds were rinsed with 2x SSC and mounted with TRIS buffer for visualization by epifluorescence microscopy. Cells were quantified as per in the contamination experiment.

Statistical analysis: Statistical analysis was conducted on the density studies in collaboration with the Biostatistics Core at University of Hawai'i John A. Burns School of Medicine. The results from the density study were evaluated with simple linear regression and F-statistic. Analysis of LDH data was performed using an ANOVA and a Tukey post hoc-test. ANOVA and post-hoc Bonferroni tests were performed on the 400,000 time course data. All data analyzed using PRISM and were only considered significant only when p values ≤ 0.05 .

2.4 Results

The aim of this chapter was to create a novel 3D culture system populated with AMC that would be more comparable to an *in vivo* environment than classic 2D culture based on cellular density, morphology, and viability. It was thought that a model more similar to the human amnion could be used in the future to study the role of these cells in the amnion and ROM.

Aim 1a: To generate a novel 3D culture system for AMC that is comparable to the in vivo based on a pure AMC population, cellular density, and morphology.

In order to determine a seeding density for the AMC into the new culture system that best reflected that seen *in vivo*, AMC from term fetal membrane explant rolls were visualized and quantified. The fetal membrane rolls showed that AMC (Figure 5) rest within the collagens of the mesenchymal layer and that upon collection there is variation as to the status of fetal membrane degradation. It can be seen that in some patients (Figure 5A, C, and D) upon collection amnion is separating from the chorion, however in other patients (Figure 5B) these layers of the fetal membranes are still adherent to each other. Quantitation of the AMC in the amnion showed that on average this layer has 5.4×10^{-4} cells/ μm^2 (Table 1).

To determine the seeding density for AMC that may be most like the *in vivo* density, cells were seeded onto scaffolds at densities ranging from 50,000 to 500,000 cells. After 24 hours (Figure 6) the lower densities (Figure 6A-D) showed very few AMC within the scaffold, while the higher densities (Figure 6E-F) appeared similar, with AMC embedded throughout the entire scaffold. Since the 400,000 and 500,000 cell densities showed AMC completely migrated within and filled the scaffold, density studies were repeated with different patient tissue. The repeat experiments at the two selected densities revealed fewer AMC within scaffold populated with patient 02 cells, at 400,000 cells per scaffold (Figure 7A) compared to cells in the same

conditions for patient 03 (Figure 7C). However, the cells placed cultured at 500,000 cells per scaffold for patient 02 (Figure 7B) also appeared sparse compared to those from patient 03 (Figure 7D). Cells at both densities from patient 02 (Figure 7A, B) are embedded throughout the entire scaffold while those from patient 03 have migrated throughout the scaffold for the 400,000 cells per scaffold density (7A), but appear to only populate half way through the scaffold at a density of 500,000 cells per scaffold (7D). Although, there was still variation, quantification of a preliminary experiment of all AMC within each scaffold was performed revealing that highest seeding density of 500,000 cells per scaffold was below that seen *in vivo* (Table 2). As variation could be seen in the way the cells populated the scaffold between patients, three further patients' cells were grown in the scaffolds for 24 hours at the same densities (Figure 8). The cells cultured at 400,000 and 500,000 per scaffold were on average of 1.54×10^{-4} cell/ μm^2 and 1.70×10^{-4} cell/ μm^2 respectively (Table 3). Simple linear regression was used to determine the effect of initial seeding density on the scaffold cell density (Figure 9) and showed that a significant relationship between initial cell seeding density and scaffold density ($p= 0.0038$), for every unit the seeding density increases, the cell density within the Alvetex scaffold of AMC will increase by 3.3×10^{-10} , demonstrating that the initial seeding density affected the proliferative behavior of the AMC.

As the data showed that the AMC are able to propagate the scaffold at the initial seeding densities, it was then necessary to compare the morphology of these cells with those grown *in vivo* and traditional 2D culture. Phalloidin/DAPI immunolabeling of AMC shows that in 2D (Figure 10A) the cells have a flattened geometry with multiple pseudopodia. All of the cells also exhibit actin stress fibers (arrowhead) and hypertrophic flattened nuclei. In comparison, the cells grown in 3D (Figure 10B) appear embedded within the scaffold, without stress fibers or

enlarged, flat nuclei. Thus, the *in vivo* characteristic fibroblast spindle shape is clearly seen when these cells are grown in 3D but not in 2D culture. When the cells are viewed in a confocal z stack, it is easy to see that the AMC grown in 2D (Figure 10C) remain flattened on single level plane, while those grown on the 3D scaffolds (Figure 10D) appear to be distributed throughout the entire width of the scaffold. Following this result, further imaging was performed to confirm the attachment pattern of the AMC within the scaffolds. It was thought that perhaps the cells had attached to one side of the pore, essentially ensuring their polarization, as in 2D. However, upon microscopic analysis the AMC were seen to attach to many sites, in multiple directions within a pore of the scaffold, forming ‘suspended’ cells (figure 11A-D).

In order to ensure that a 3D model was being developed that would be able to answer questions about AMC behavior the purity of the cells isolated and placed into the scaffolds was also tested. Vimentin immunocytochemistry of AMC (figure 12) showed a 1.3% contamination rate of cultures with AEC.

Aim 1b: To determine the effect of time on AMC density in culture

With the cells at the 400,000 and 500,000 cells per scaffold seeding densities appearing similar, there was concern regarding the time dependent characteristics of these cells. Therefore, a time course study was performed with cells at these seeding densities showing a significant level of cell proliferation over time. An initial time course was performed using AMC from Patient 04 with the initial seeding density of 400,000 cells (Figure 13A-G) that showed an initial single monolayer of AMC that resolved as the cells migrated through the scaffold by day 7. Three further patient’s cells were also looked at over time and it could be seen that each patient’s cells behaved differently. In each of the 400,000 initial cell seeding density time course experiments, a monolayer was noted (Figure 13A, H, K-N, O-R) that appeared to resolve

(Figure 13I-J) or was maintained through the entire the completion at 7 days (Figure 13K-N, O-R). However, when quantification of the AMC within scaffolds at the 400,000 cell density did not reach similar values of cell number to that know to be in this layer of the fetal membranes, the time course was repeated with 500,000 cells per scaffold. The initial 500,000 cell per scaffold time course study (Figure 14) used AMC also from Patient 03 (Figure 14A-D) and showed an absence of a cell monolayer, but a larger layer where AMC appear to have not migrated throughout the scaffold. By day 3, AMC were noted through the scaffold, but with what appears to be two peripheral monolayers (Figure 14-D). A loss of cells was seen on day 5, as well as a single monolayer on one side of the scaffold, that continued to the 7 days in culture tested. A repeat of the 500,000 cells per scaffold time course (Figure 14E-F) also showed that AMC remained on one side of the scaffold on day one, but that they fully migrated into the scaffold by the completion of the time course on day 7 where two monolayers could also be seen on either edge of the scaffold. These results taken together with the earlier time course experiments, patient to patient variation is evident in terms of when cellular migration occurs and day of proliferation. Thus, closer examination of the monolayers appearing throughout the numerous time course experiments, were undertaken to decide if their morphology could be qualitatively assessed. Upon close examination cells of the monolayer appeared to be more cuboidal in shape with close connections to one another (Figure 15).

Since the initial seeding densities of 400,000 and 500,000 cells per scaffold at 24 hours did not yield a density similar to that seen in this layer of the amnion in the fetal membrane density, the AMC within the scaffold time courses grown over a week. Quantification of the 400,000 cell per scaffold time courses (Figure 16) showed that the total number of AMC within the scaffolds increased over the course of the culture, as evidenced by, an average of 50%

increase in cell density. However, none of the patients reached the *in vivo* goal, averaging only about half of the *in vivo* average. Pooled patient data (Figure 16D) shows that there is a significant difference in cell density over time in culture ($p=0.0130$) providing evidence for proliferation. The data collected from the quantitation of the time courses where the cells were seeded at 500,000 cells per scaffold did show that the cells from one patient reached a density comparable to that seen *in vivo* (Figure 17B), however, the other patients cells (Figure 17A) appeared not to proliferate as robustly. Therefore, the pooled data from these experiments show an increase in cell density over the week in culture that seems more similar to *in vivo* than that seen for cells cultured at 400,000 cells per scaffold over a week (Figure 16D). Therefore, from these results it was determined that a density of 500,000 cells per scaffold would be the most informative seeding density to use in this model as it is closer to the *in vivo* density.

Aim 1c: To measure the Cell Survival Characteristics of AMC in 3D culture and compare them to 2D culture

To evaluate if necrosis occurred in the 2D and 3D AMC culture models, propidium iodide incorporation was utilized to visualize dead cells (Figure 18). It was noted during visualization that the PI had leached from the cells and had collected outside the nucleus (Figure 18A). However, although full analysis could not be performed, upon initial viewing no PI incorporation was noted in culture system in any samples except the positive control.

To determine if AMC grown in either 2D or 3D culture models exhibited cell death leading to cell lysis, the cytotoxicity level of each system was evaluated by a LDH assay (Figure 19). AMC cultured from patient 03 (Figure 19A) showed little variation in the level of cytotoxicity between 2D and 3D models, as it remained low and fairly steady. For those cells

grown from patient 06 (Figure 19B), the initial 2D seeding appeared to have a higher level of LDH compared to the later days of 5-7. However, in contrast the cells grown in 3D from patient 06 started low, but increased over the full week of the time course. The AMC from patient 07 (Figure 19C) showed a steady rate in 3D over the 7 days in culture, but in 2D the cells showed an increase starting around day 6. Despite the small differences between each patient's cells' behavior there was no significant difference in the levels of LDH secreted between those cells grown in 2D and 3D throughout the duration of 7 days.

2.5 Discussion

The purpose of this study was to create a novel 3D culture system for AMC that is comparable to *in vivo* to provide a more similar method of studying the amnion and ROM. This study produced the first attempt at making a 3D system specifically for ROM research as others using AMC in 3D have only attempted to produce models focused on tissue engineering purposes (Bilic *et al.* 2005; Rodriques-Fuentes *et al.* 2015). Overall, the results showed that AMC within the Alvetex scaffold can; migrate, proliferate, and have a morphology that is similar to *in vivo*, with little cell death. However, a comprehensive comparison is still needed to be completed to increase confidence in this new 3D culture system, as currently many of the viability experiments remain incomplete or inconclusive.

As part of the normal aging process of the fetal membranes, in preparation for labor and delivery, weaken and the layers of the amnion and chorion separate from each other (Arikat *et al.* 2006). From those tissues collected from the patients included in this study, it could be seen that there was variation in the gestational status and proximity to labor due to the collection window being between 39-42 gestational weeks. This was exemplified by those fetal membrane sections that demonstrated differing degrees of amnion and chorion separation (Figure 5). This variation

in patient tissues can also be seen in the behavior of the cells isolated from this tissue. The time course and cell density experiments, showed that cell migration times and proliferation rates were also different depending on the patient. Not only do the differences in gestational age affect the amnion/chorion integrity but in addition, changes in proximity to labor can clearly affect the ability of cells isolated from this tissue to grow well in culture; the closer they are to labor, the less proliferation is seen and thus those that are lost due to apoptosis are not replaced (Parolini *et al.* 2008; Khwad *et al.* 2004).

Previous studies using mesenchymal cells on Alvetex scaffolds have used an initial seeding density of 1 million cells per scaffold (Reinnervate ReproCell 2015). However, it was not feasible to replicate this number in this study, as it is not possible to obtain this number of AMC due to the absolute numbers of viable cells in this tissue layer at the end of pregnancy. Therefore, to propagate enough cells to be able to have a reasonable number for multiple condition experiments, the AMC were grown in 2D culture, up to 4 passages. The fact that these cells proliferate slowly (Parolini *et al.* 2008) and cease proliferation at the end of gestation may well play a part in their limited supply *in vivo*. Therefore, the selection of seeding densities to evaluate Alvetex as a 3D model to grown these cells in, was challenging and not logistically feasible a densities higher than 500,000 cells per scaffold. During the 24 hour density experiments, none of the tissues matched the density quantified in the fetal membranes, but this was considered to be desirable because a dynamic model was needed in which the AMC needed space to proliferate and fill the scaffold over time. This allows this model to become potentially valuable for dynamic mechanistic downstream assays overtime. Although the 400,000 and 500,000 cells per scaffold seeding experiments showed similar results after 24 hours, the 500,000 cell density, according to the proliferation data, not only yielded a density closer to that seen in

the fetal membranes at the end of gestation after the week in culture but also proliferated at a higher rate. This is perhaps an indication of their wellbeing in the scaffold, as other studies have noted a higher proliferation rate of AMC in 3D culture (Rodrigues-Fuentes et al. 2015). In addition, based on the simple linear regression model (Figure 9), to match fetal membrane density in the Alvetex scaffolds on day 1 around 1.6 million cells would be needed to be seeded, which is unobtainable immediately upon tissue isolation and it is also not feasible to expand the AMC populations in 2D to reach this number, as their proliferation rate rapidly decreases after passage 2.

One of the most notable and easily witnessed issues endemic to 2D culture is the force polarity it enables cells to acquire (Shamir, Ewald 2014). However it appears that this does not occur to AMC within the 3D scaffold, as it can be seen from the results that they did not have an apparent polarity and maintained a fibroblast like shape. This phenomenon of AMC reverting to their original shape when seeded in 3D cultures is well documented, where they take on a 2D morphology but immediately resume their *in vivo* shape when transferred to another environment (Rodriguez-Fuentes et al. 2015; Bilic *et al.* 2005). Numerous stress fibers, which consist of actin and myosin, are visible within AMC when grown in 2D culture. These are not only indicative of cellular stress, but also definitive of cell adhesion differences between 2D and 3D culture models (Grinnell 2003). The confocal Z stack images of AMC morphology (Figure 10) were able to demonstrate that the cells were able to migrate to a location deep within the scaffold. In 2D, AMC were restricted to a flat monolayer, which is clearly contrary to those in the 3D scaffold. This difference is thought to be due to the abundance of pores composing the Alvetex scaffolds that allow more opportunities for AMC to make contact and adhere in multiple directions. Closer examination of these adhesion locations (Figure 11) showed that AMC are able to make

multiple adhesions around a pore to fill the voided space and ‘suspend’ themselves within the pore. Similar adhesions are not seen in 2D culture where AMC tend to become spread uniformly compared to a spindle formation seen in 3D. The differences in morphology between the two culture systems is valuable because cell geometry has been linked to alterations in cellular function like ability to differentiate, sensitivity to apoptosis (Baker, Chen 2012; Weaver et al. 2002), gene expression pattern (Knight, Przyborski 2014), and even types of cell adhesions that the cells exhibit (Cukierman et al. 2001). These differences could reveal novel concepts regarding ROM, which were previously unobtainable in 2D culture due to their inappropriate phenotype.

The contamination rate of AEC measured within the novel 3D system was lower than the reported average of 2%. However, any contamination of AEC can lead to changes in AMC behavior and alter the gene expression results and, therefore, it is crucial to continue with developing a better cell isolation method for a strictly pure population of AMC for future research with this model. It was initially believed that the AEC contamination would decrease with successive media changes and passages as they typically require 4 days to adhere in culture. It is unclear if the AEC contamination rate changes with each passage in our culture model. However, as other studies have described AMC acquiring an AEC phenotype in culture (König et al. 2014) via mesenchymal-epithelial transition (MET), it is possible that the presence of AEC in these culture experiments could derive from MET. Future assessment of AEC presence after each passage would provide an indication as to MET and/or initial contamination contributed to the presence of AEC with this 3D model.

The initial monolayer of cells resting on one surface of the scaffold, was seen on day 1 or 2 in some patients indicates that this cellular behavior is most likely a migration issue. This is

because it is thought that they cells remained in their initial seeding position and is supported by the resolution of this phenomenon after 3 days in culture. It is not clear why some patient's cells need more time to migrate through the scaffolds, but it may be due to the proximity of labor at the time of cell collection or individual patient to patient variation. Closer examination of the later monolayer showed a distinct difference in cellular morphology in some scaffolds compared to the rest of the cells within the scaffold, suggesting that they are epithelial cells. Although, yet to be confirmed as epithelial cells, one possible explanation for such is the contamination of AEC as addressed above. To confirm this observation, further experiments need to be performed by testing for epithelial and mesenchymal cell lineage markers (for example E-cadherin and vimentin) by Immunocytochemistry. If MET is confirmed, this novel 3D model will provide an invaluable *in vitro* tool to simulate amniotic membranes.

By performing two different density time courses, the recapitulation of *in vivo* numbers of AMC was attempted. Over the course of 7 days, the 400,000 cells per scaffold time course did not reach the desired density, however those seeded at 500,000 per scaffold were very close to the goal (6% lower). Since these experiments were only performed over the course of 7 days, it is reasonable to expect that leaving AMC in 3D culture for longer would yield an exact *in vivo* match. An *in vivo* density match would further support this model as an *in vitro* way to study the amnion because density has an effect on cell survival characteristics, therefore, to understand a true representation of AMC behavior the density needs to be matched. Also, as the polystyrene scaffold is not biodegradable, the AMC could be cultured over longer periods of time to give an opportunity for the cells to proliferate enough to mimic the *in vivo* density. Continuation of this work should aim to show how AMC behave over longer periods of time and if they start to secrete their own ECM to fill the scaffold pores. An important aspect of the time course

experiments is that they showed an increase in cell density as the experiment progressed. This is solid evidence that AMC are able to proliferate in the novel 3D system, at least once on average within 7 days. However, further studies need to be completed to calculate the rate and magnitude of proliferation, this could be performed by MTT or almarBlue assay.

Although some cells are clearly viable in the novel 3D system, the exact levels of cell survival, proliferation and death are as yet undetermined. If this work were to be continued, it would be important to evaluate the rate of apoptosis and perform quantitative proliferation studies to fully validate the novel culture system. The evaluation of the level of hypoxia in the 3D system versus the 2D would also be interesting to complete, although the degree to which the amnion during gestation experiences hypoxia remains uncertain.

The propidium iodide experiments were unable to provide quantifiable results, due to the leaching of this marker from the cell. As other studies have shown a drastic decline in the ability of cells to retain PI after incorporation, lasting only a few hours to a few weeks (Falzone et al. 2009; O'Brien, Bolton 1995) depending on the cell type. It is unclear when exactly the PI leached from the cells in the experiments performed in this study, but it occurred within two weeks, which is within the known window for its dissipation characteristics. Further studies using PI, documenting its incorporation in AMC need to be completed to determine the levels of dead cells in the culture conditions. However, the levels of necrosis and apoptosis can be somewhat assessed by the consideration of the levels of cytotoxicity by LDH secretion, which did not differ between 2D and 3D. This data supports low levels of necrosis/apoptosis in the novel 3D system. Interestingly, two of the patients' AMC paralleled the levels of LDH activity with their proliferation characteristics. Close examination showed that AMC appeared to proliferate between day 5 and 6 in Patient 03 when the LDH activity decreased showing that

once the occurrence of cytotoxicity is low, the AMC then tend to proliferate. This was also noted in the cells of Patient 07. However, more studies evaluating proliferation characteristics, like an MTT assay, coinciding with another LDH assay need to be completed to be definitive.

In conclusion, the data from Aim 1 supports the hypothesis that culturing AMC within the Alvetex scaffold yields viable cells and a novel 3D model for this layer of the amnion. This is based on the obvious ability of these cells to proliferate and their low levels of LDH secretion and activity. A full comparison of the 3D model to 2D culture is still ongoing and requires the completion of other viability assays before definitive conclusions regarding the scope of this model can be made. Although the complete characterization of the new AMC 3D tissue model is yet to be completed, many of the key experiments performed in this study demonstrate the validity of the model generated in this aim. In addition, according to the results generated here, it can be concluded that there are distinct differences in the cellular morphology of AMC when grown in 2D and 3D as predicted by the hypothesis. In addition, although the cell density of the fetal membranes was not matched exactly, but given more time in culture, it is likely the AMC density of the scaffold can mimic that of the membranes and be a valuable recapitulation of this layer of the amnion for future studies that aim to understand the mechanisms of ROM.

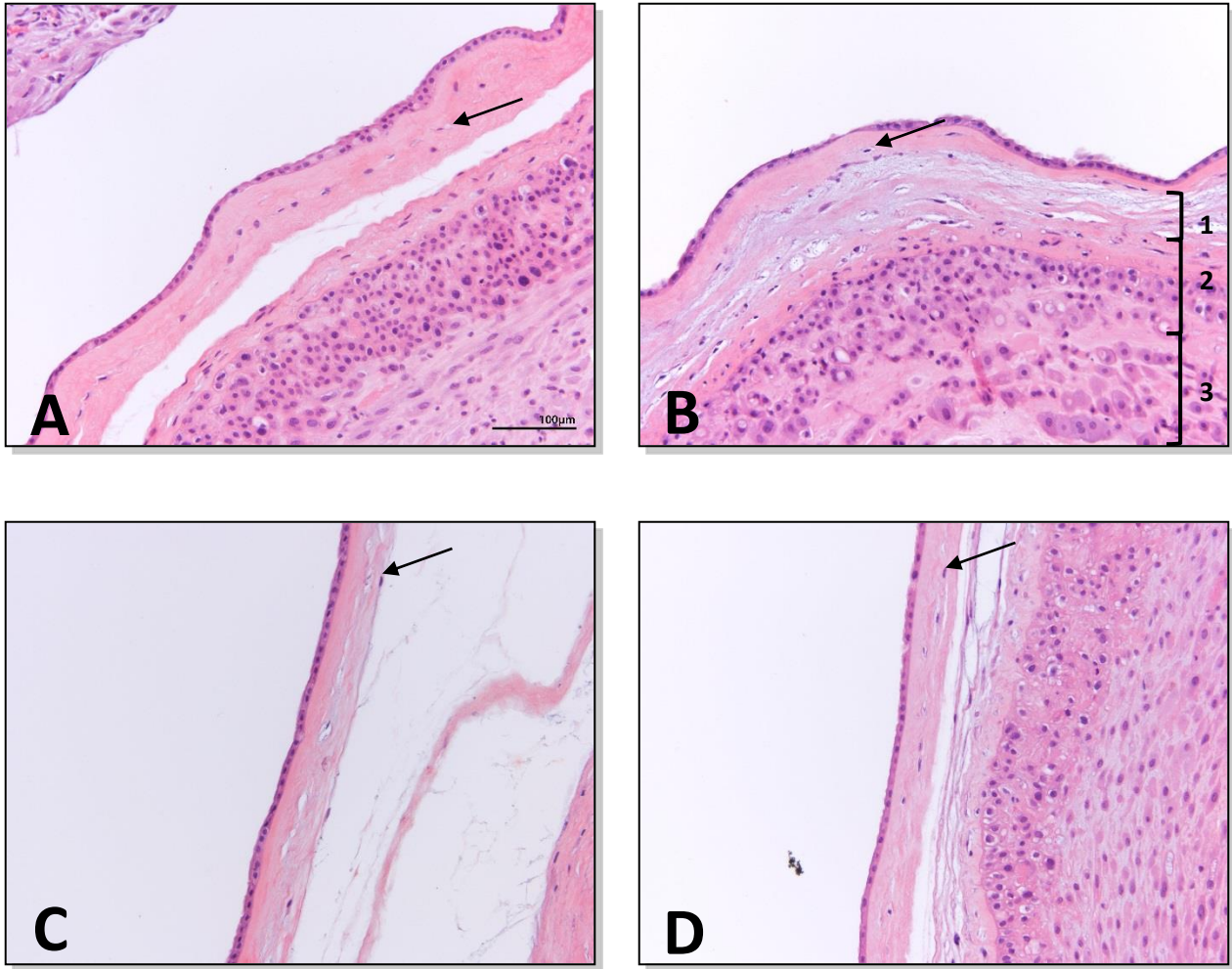


Figure 5. H&E stain of human fetal membrane (20x). Tissues were collected from 4 patients (A-D). Layers of amnion (1), chorion (2), and decidua (3) are indicated and AMC within the amnion indicated by arrows.

Cells/μm^2 in Fetal Membrane (n=6)	
Average	5.4×10^{-4}
Standard. Deviation	9.3×10^{-5}
Standard Error of the Mean (SEM)	7×10^{-2}

Table 1. Quantification of AMC within human fetal membranes in cells/ μm^2 .

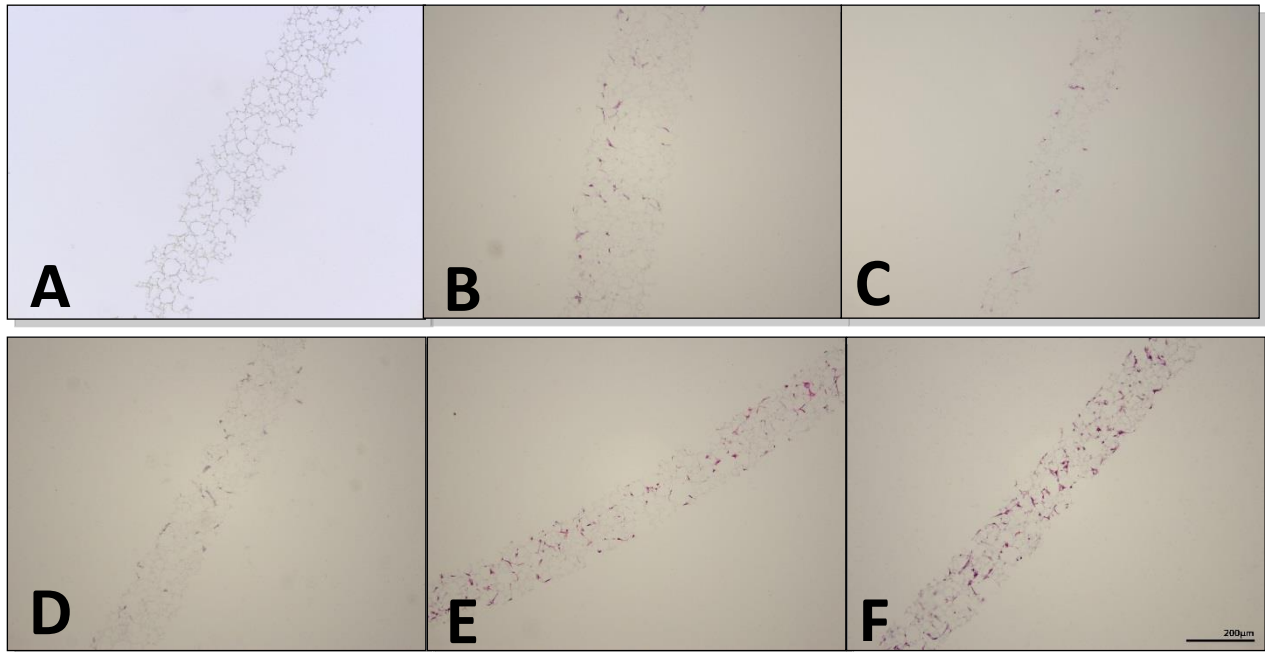


Figure 6. Seeding densities (A) 50,000, (B) 100,000, (C) 200,000, (D) 300,000, (E) 400,000, and (F) 500,000 cells per scaffold of AMC from Patient 01 at 10x after 24 hours in culture and stained with H&E. Scale bar 200µm.

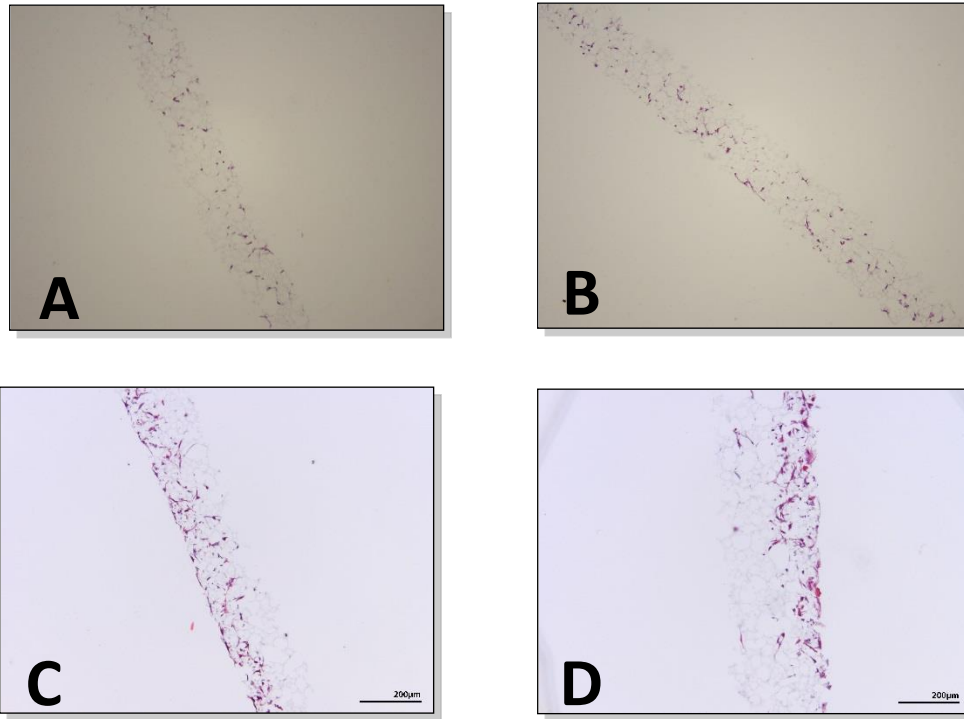


Figure 7. Seeding density of AMC from Patient 02 at 400,000 (A) and 500,000 (B) and Patient 03 (C) 400,000 and (D) 500,000 and stained with H&E. Scale bar 200µm.

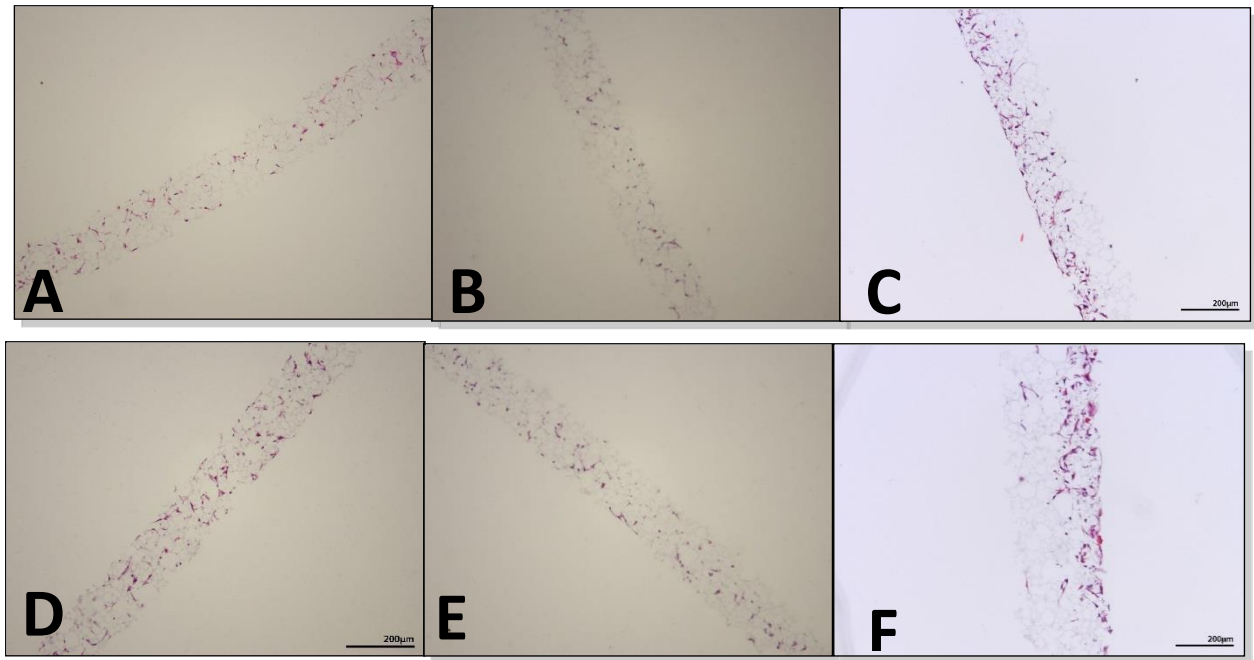


Figure 8. Seeding densities of AMC 400,000 from three different patients (A,B,C) and 500,000 (D,E,F) (10x). Stained using H&E of AMC in Alvetex scaffold after 24 hours in culture.

AMC P01 Seeding Density	Cells per μm^2 after 24 hours
50,000	0
100,000	0.48×10^{-4}
200,000	0.50×10^{-4}
300,000	0.62×10^{-4}
400,000	1.16×10^{-4}
500,000	1.73×10^{-4}

Table 2. Quantification of cell density seeding experiment with AMC from Patient 01.

Tissue	Cells per μm^2 after 24 hours			Average
	P01	P02	P03	
400,000	1.16×10^{-4}	0.99×10^{-4}	2.47×10^{-4}	1.54×10^{-4}
500,000	1.73×10^{-4}	1.05×10^{-4}	2.29×10^{-4}	1.69×10^{-4}

Table 3. Quantification totals of AMC density study after initial seeding of 400,000 and 500,000 cells per scaffold from 3 patients.

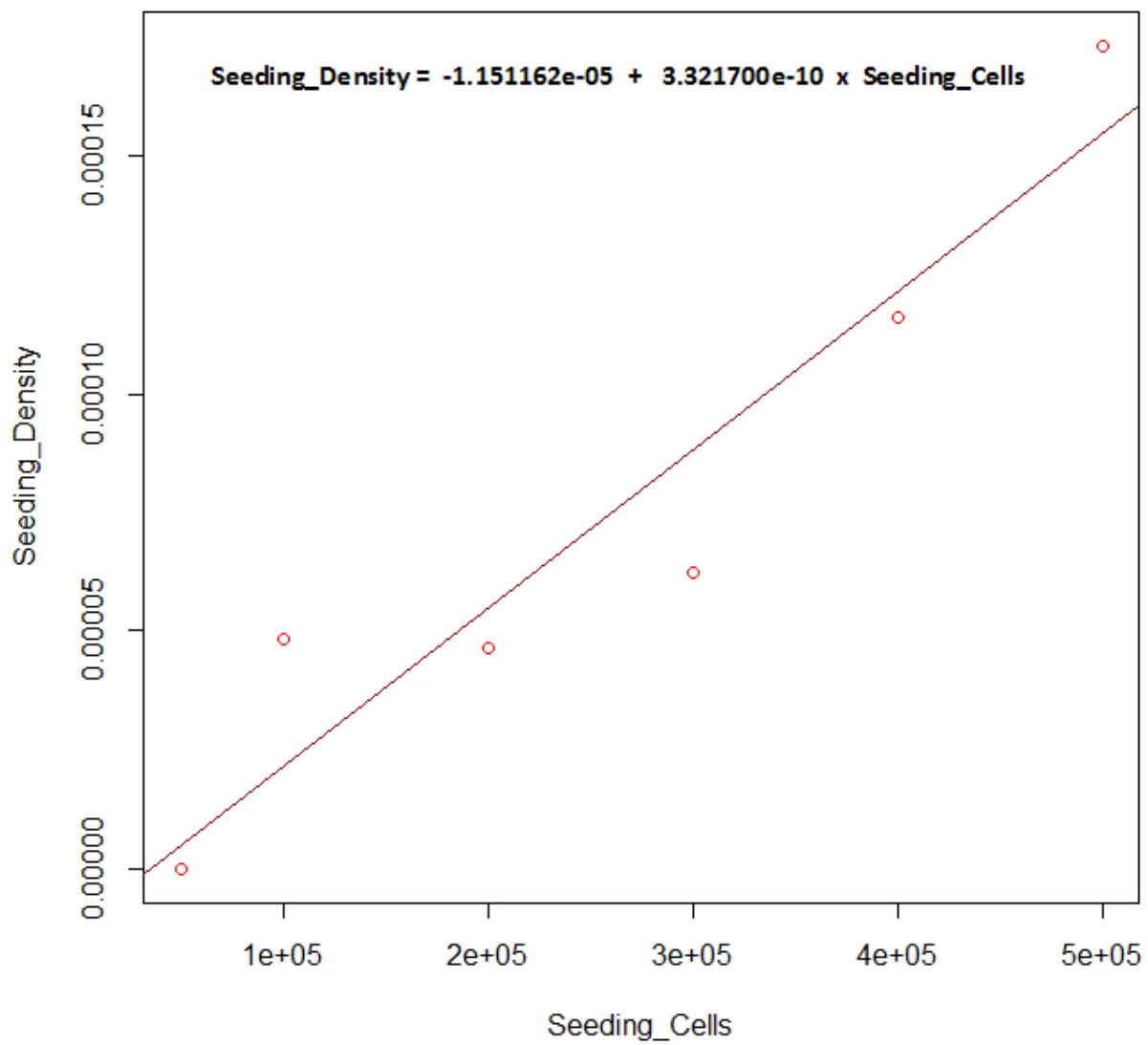


Figure 9. The correlation between seeding density and change in number cells.

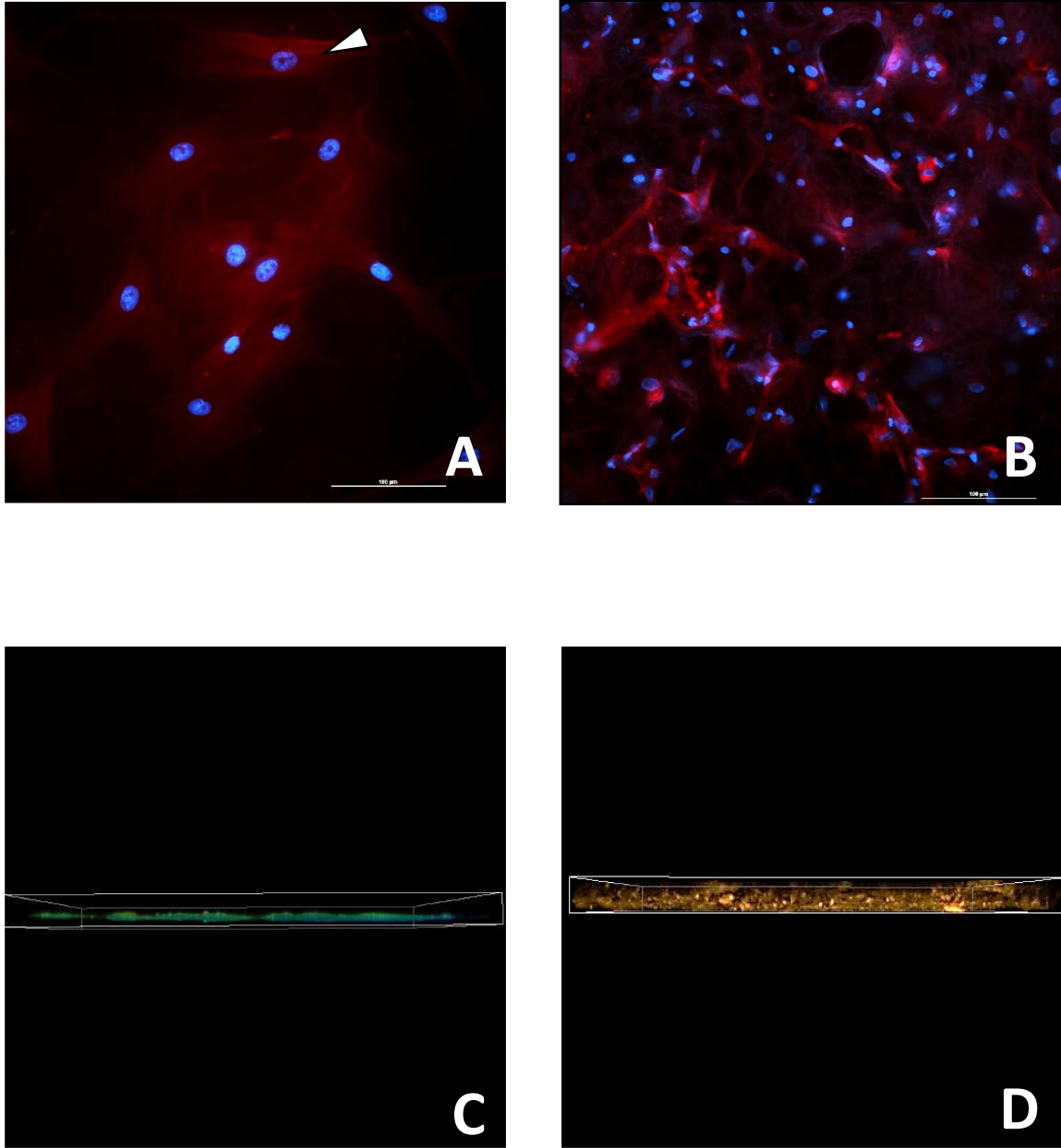


Figure 10. Phalloidin (red)/DAPI (blue) label of AMC in 2D (A) and 3D (B) imaged with epifluorescence (20x). Confocal Z stack of AMC phalloidin label in 2D (C) and 3D (D) (20x). Scale bars 100µm.

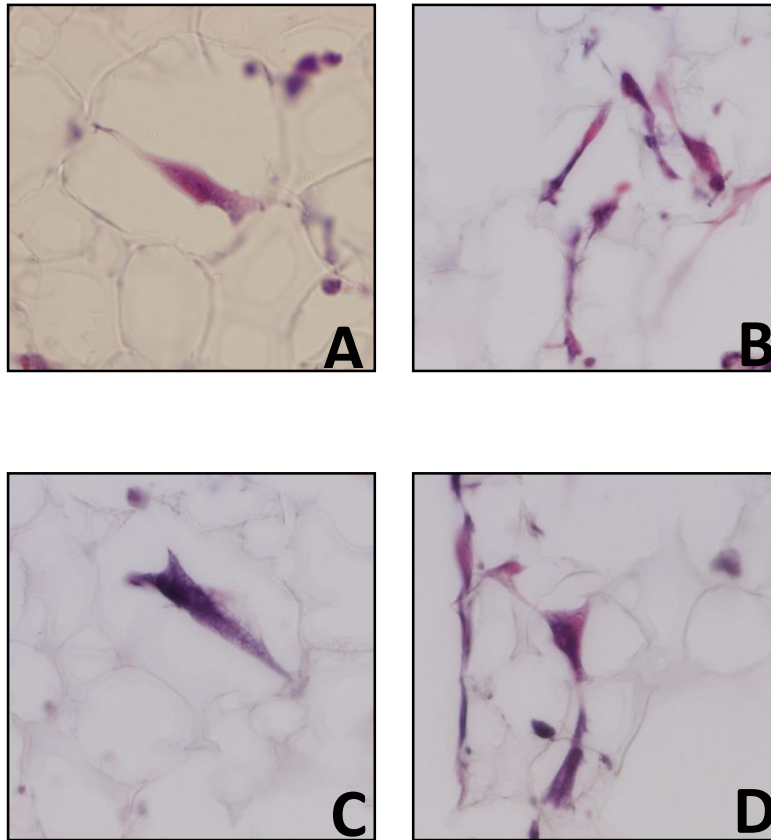


Figure 11. Four examples (A-D) of H&E staining of AMC within Alvetex scaffolds viewed (60x).

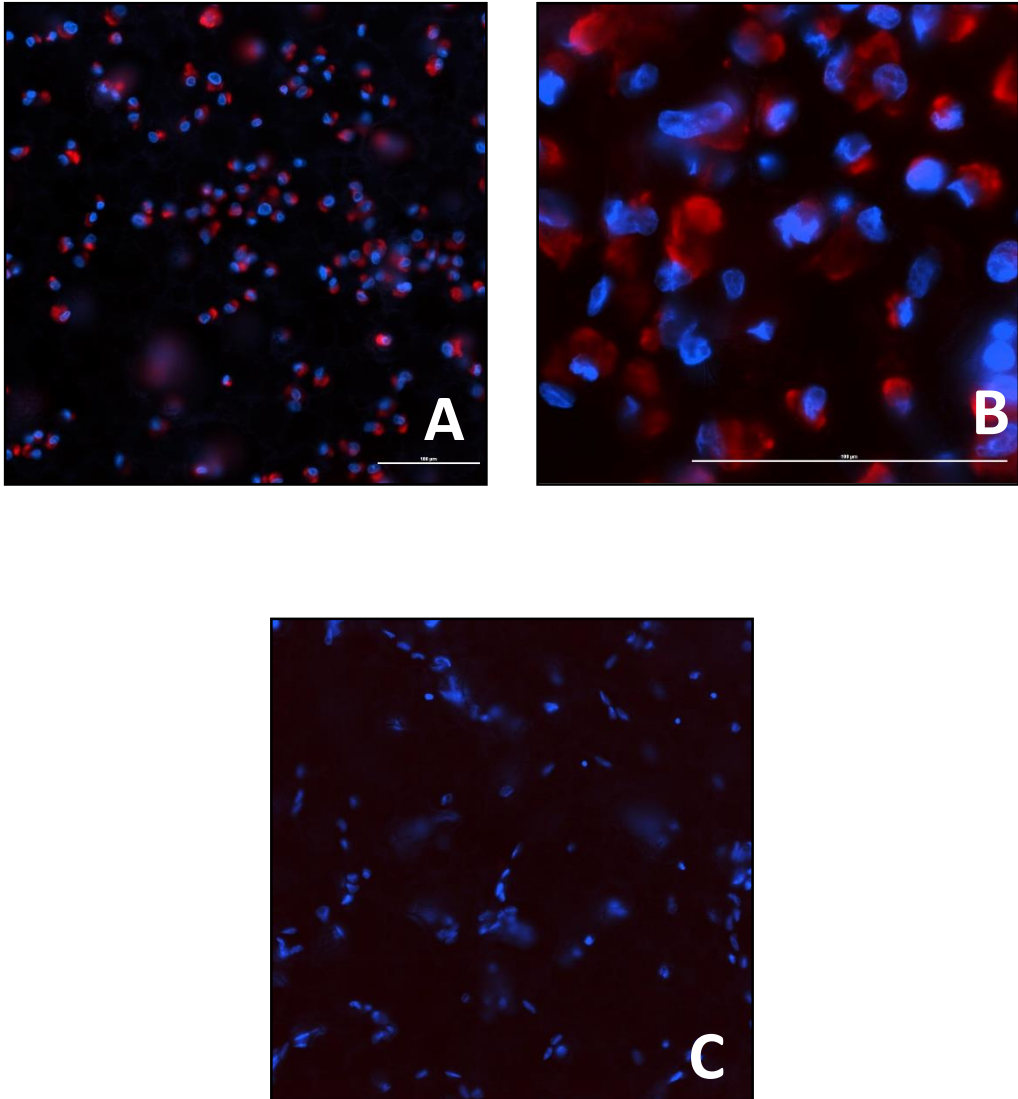


Figure 12. Vimentin (red) and DAPI (blue) label of AMC in 3D shown at 20x (A) and 60x (B) with scale bar 100 μ m and negative control (C) was void of a primary antibody (20x).

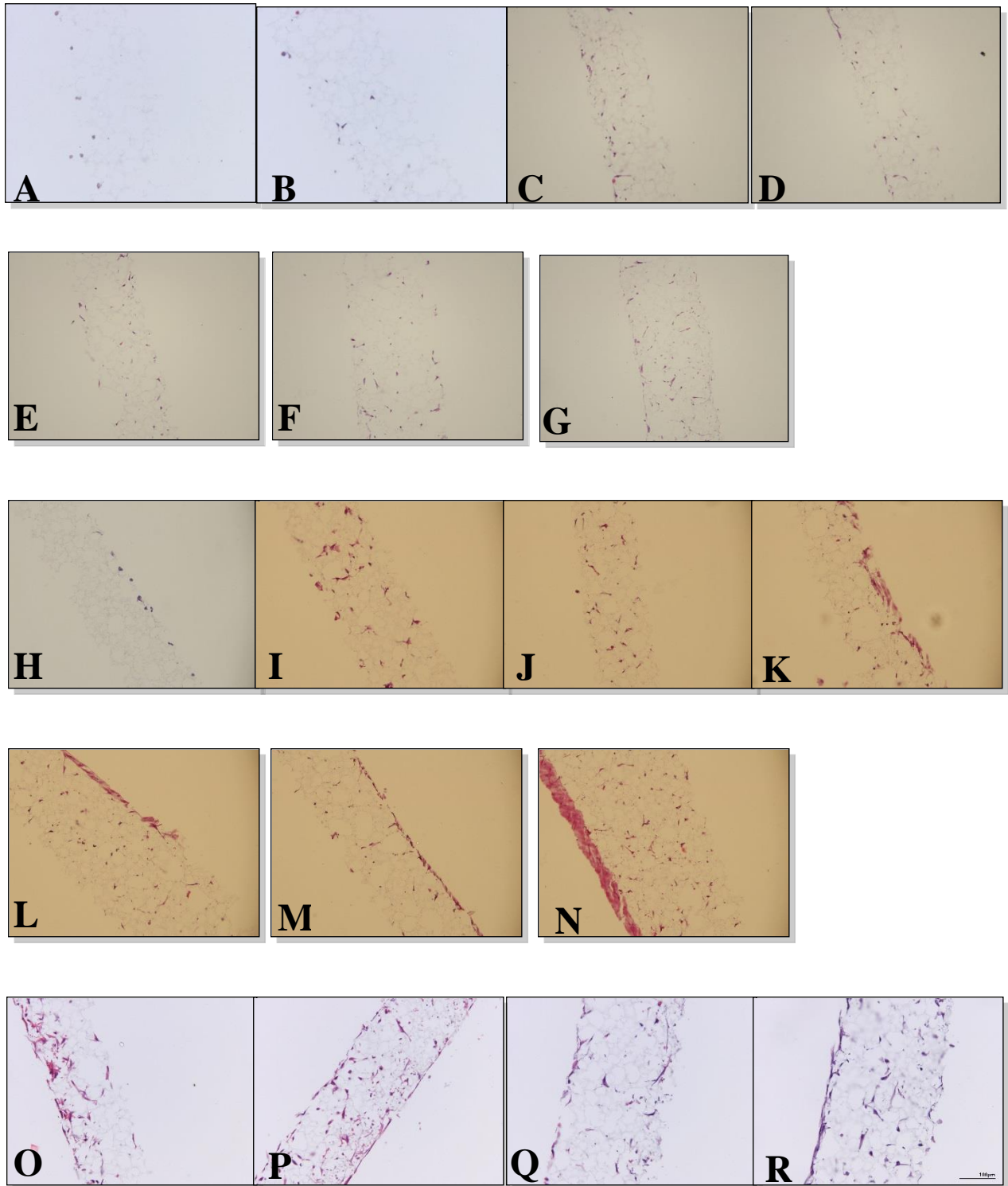


Figure 13. H&E stain of AMC placed in Alvetex scaffold at 400,000 cells per scaffold for 7 days (1-7) from tissue P04 (A-G), P05 (H-N) and days 1, 3, 5, and 7 for P03 (O-R).

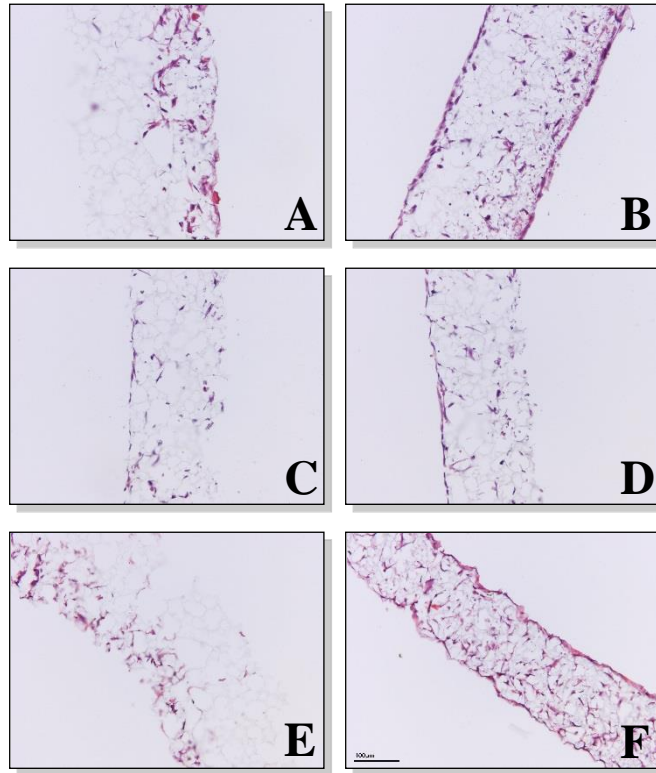


Figure 14. H&E stain of AMC placed in Alvetex scaffold at 500,000 cells per scaffold over 7 days (1, 3, 5, and 7) from Patient 03 (A-D), and days 1 and 7 for Patient 07 (E-F). Scale bar 200 μ m.

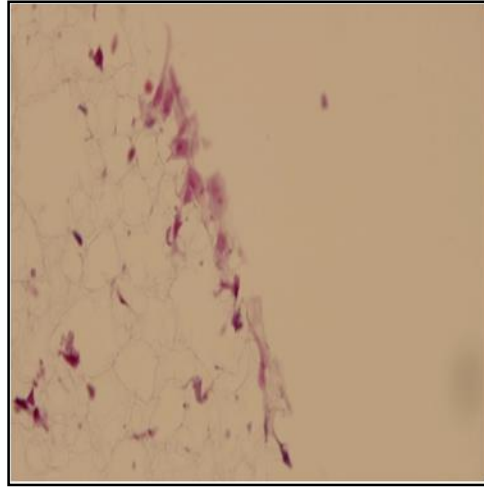


Figure 15. H&E stain of AMC in Alvetex seeded at 400,000 cells per scaffold and grown in culture for 4 days (40x).

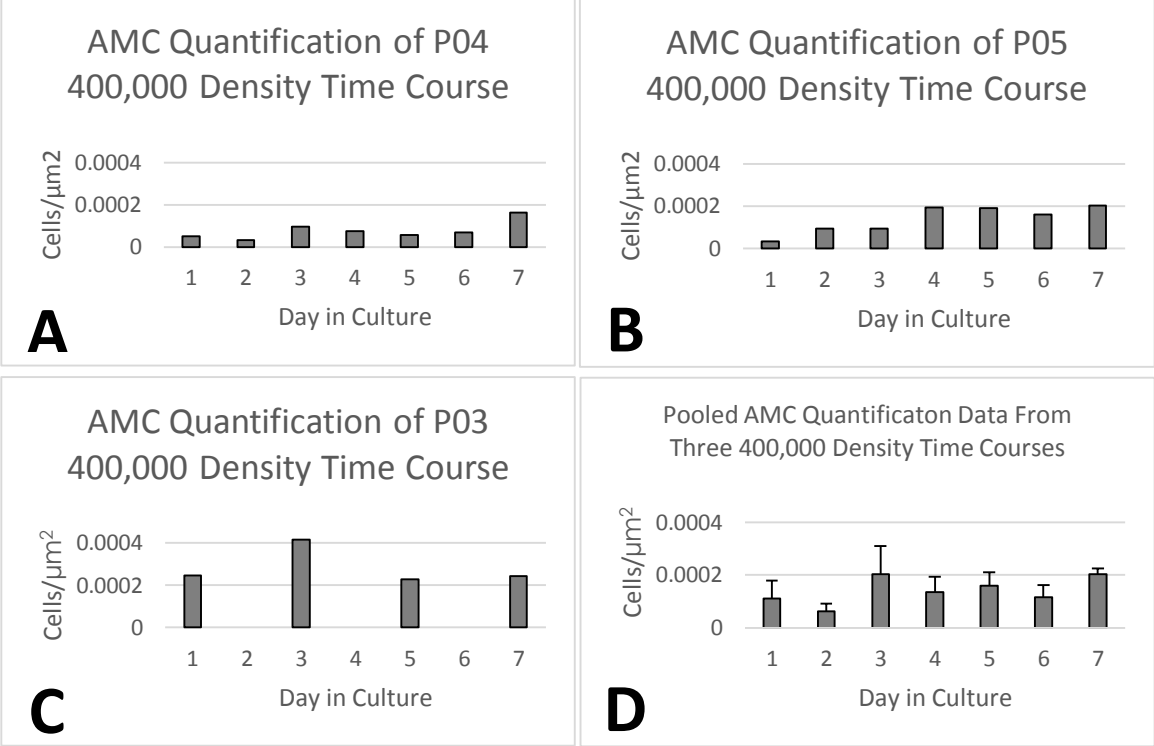


Figure 16. A-C represent AMC grown at 400,000 cells per scaffold from 3 separate patients and (D) pooled data from the patients. Error bars represent SEM.

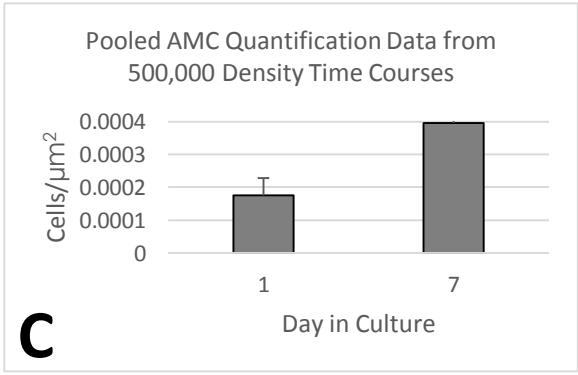
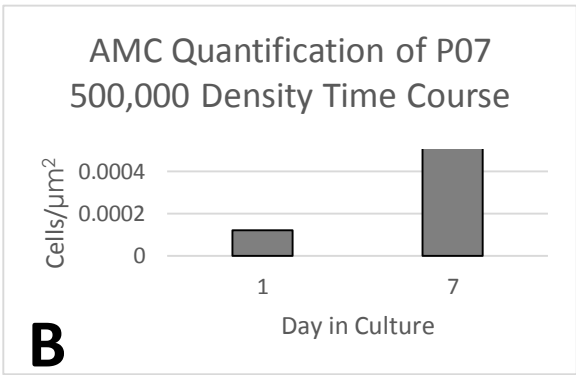
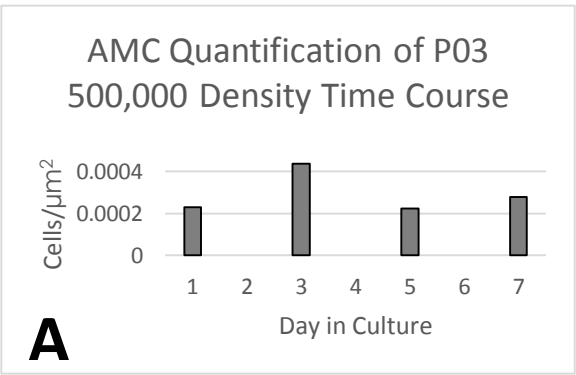


Figure 17. A-B represent AMC grown at 500,000 cells per scaffold from 2 separate patients and (C) pooled data from the patients. Error bars represent SEM.

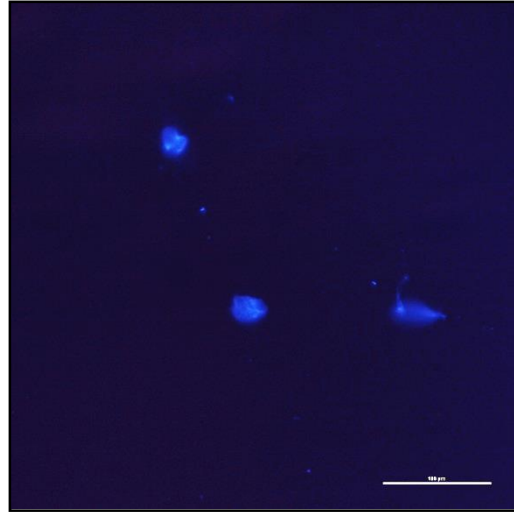
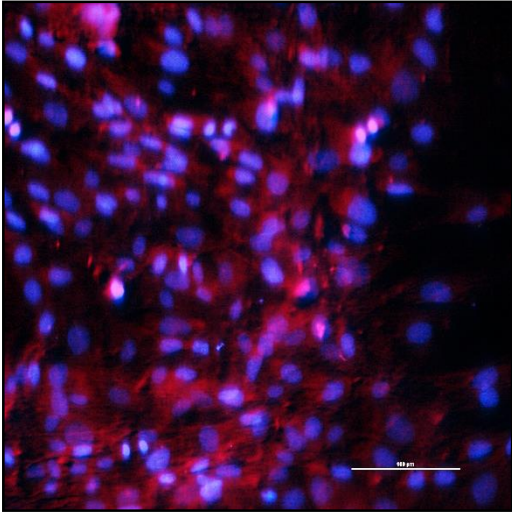


Figure 18. Propidium iodide (red) label of AMC depicted in 2D with DAPI nuclear stain (blue) after 7 days in culture. Scale bar 100 μ m.

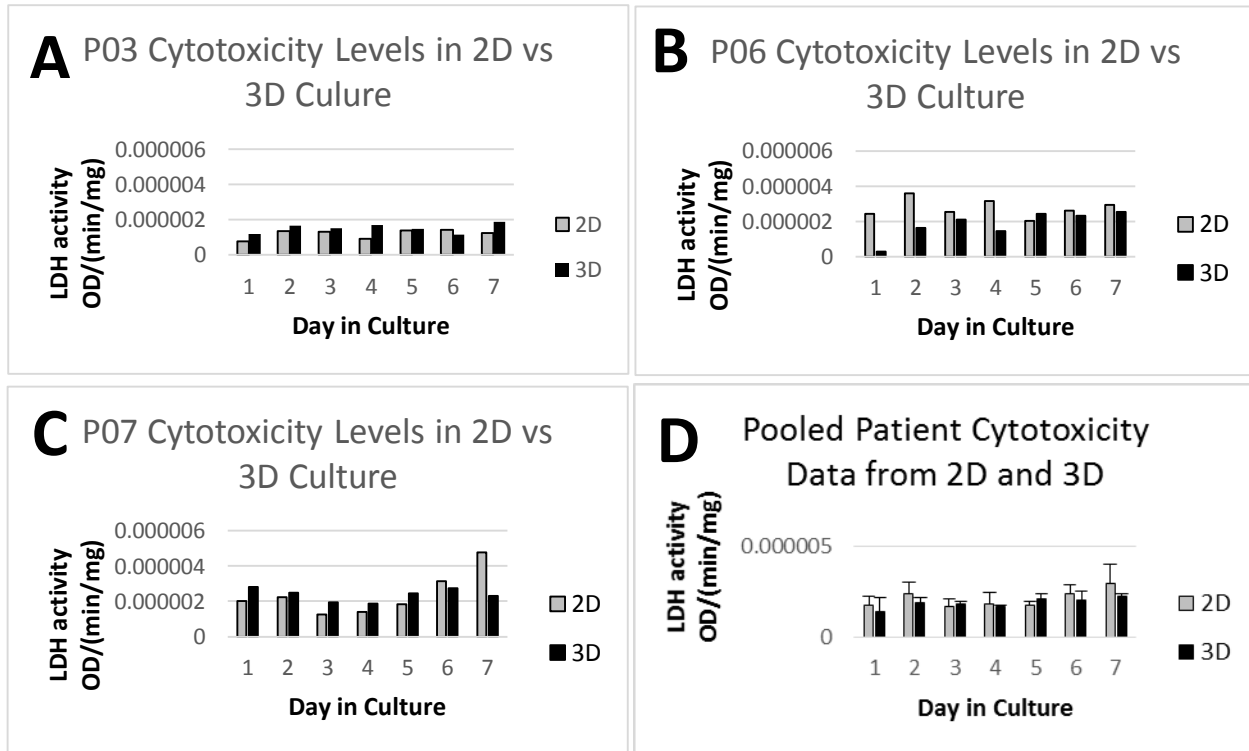


Figure 19. LDH secretion from AMC grown in 2D and 3D from tissues Patient 03 (A), Patient 06 (B), and Patient 07 (C). Pooled data from all patients (D). Error bars represent SEM.

3.1 Introduction

Typical 2D culture is known to force cells to express an apical-basal polarity altering cell to cell and cell-matrix adhesions that can modify gene expression (Shamir, Ewald 2014; Knight, Przyborski, 2014), yielding altered expression patterns *in vitro* versus *in vivo*. The fact that cells are able to change their behavior like this, means that research performed on AMC to understand ROM may generate data, from isolating and culturing these cells in 2D, that does not reflect how these cells would behave *in vivo* or if grown in a 3D environment. 3D cell culture is a way of generating an environment that is more similar to that seen *in vivo* and has been shown to produce cells that behave and grow in a similar physiological state, once embedded. This is thought to be because when grown in 2D, cells are limited to a linear form that often alters their function, as many cells require contact with surrounding cells in the tissue or surrounding ECM for correct signaling. Although when grown in 2D cells react to that environment and take on specific morphology and behavior based on the environmental cues, some cells have been seen to regain a more *in vivo-like* phenotype once placed into a 3D environment. For example, dedifferentiated chondrocytes restored their cellular shape and their classic expression of cartilaginous cell-specific markers once encapsulated in 3D (Baker, Chen 2012). Other studies have directly compared lung fibroblasts grown in 2D vs a 3D collagen gel that resulted in clear morphological differences, illustrating that once placed into a 3D environment, the cells appeared to look similar to those from an *in vivo* environment as their pseudopodia did not appear flattened and fan-like as seen in 2D (Elsdale, Bard 1972).

Culturing cells in 2D and 3D environments has also shown behavior differences not just in morphology, but also in migration, proliferation, differentiation, matrix remodeling, and cell-

matrix interaction formation; all processes vital to cellular function. One of the important considerations for cells that are to be utilized in tissue engineering and cancerous tumor generation, is that the cells used are able to differentiate into a desired form, often working in concert with other cell types. In breast cancer research, human mammary fibroblasts grown in 3D were seen to have an increased level of paracrine signaling molecule secretion that catalyzed the transition from *in situ* to invasive carcinoma when compared to those cells grown in 2D cultures (Sung *et al.* 2013) rendering 3D an important *in vitro* model for increasing understanding of what occurs *in vivo*. Differences in cellular behavior, have also been noted when cells are grown in the Alvetex scaffold. Rat mesenchymal cells grown on the Alvetex scaffold and induced into osteogenic cells, showed an enhanced osteogenic differentiation, complete with more calcium deposits versus a 2D comparison (Reinnervate 2015). The differences seen between 2D and 3D models stem from the changes in cell adhesions that mediate cellular behavior. It is thought that these changes in cellular behavior in 3D culture stem from the scaffold allowing for more multi-directional cellular attachments.

It has been well documented that when grown in 2D, cells exhibit cell-matrix adhesions that originate with a focal complex that evolves to a focal adhesion, and then a fibrillary adhesion. In each type of adhesion, there are specific components that can be used to identify classify the adhesion type. For example, focal adhesions contain paxillin and $\alpha_v\beta_3$ integrin while fibrillar adhesions contain fibronectin and $\alpha_5\beta_1$. However, all of these proteins are essential for cell-substrate adhesion allowing the bidirectional transmission of cell signaling. Another type of adhesion has been identified, called a 3D adhesion, that is characterized by components of both focal and fibrillary adhesions; paxillin, α_5 integrin, and fibronectin (Cukierman *et al.* 2001). Questions regarding the driving force behind the differences in the protein expressed in these

different types of adhesion, what dictates which proteins are expressed and when, and also if these changes lead to differences in cellular signaling behavior, all remain areas of active research in this field.

Given that there is a clear difference in cellular adhesion expression seen between 2D and 3D culture, and knowing that cell-matrix interactions govern many important cell functions, it may become imperative to improve our understanding of cellular behavior driven by environmental cues. This would help to complete a more comprehensive evaluation the cell adhesion expressions of cells grown in 2D and 3D. One way to evaluate the status of a cell is by the study of its gene expression transcripts. Evaluation of full transcriptomes in 2D and various tissue samples have already revealed functions for numerous novel transcripts that were previously unknown for neovascularization, neuronal gene promoters, and cancer metastasis (Rienzo et al. 2014; Hu et al. 2014; Zhao, Li, et al. 2014). Therefore, these studies revealed new transcripts that added new targets for study in their respective fields of biology. The same strategy could provide vital new information regarding the normal processes of ROM, since much about AMC and the amnion remains unknown. Evaluation of transcripts in these cells could also help to improve understanding of the normal ROM mechanisms that are dysregulated leading to PPRM.

With the constantly expanding knowledge of complex systems, driven by 3D cell culture technologies, there is ample opportunity for the expansion of research on cell-matrix interactions and their role in cellular behavior. This may be due to the ability of cells to make multiple adhesions in a variety of dimensions ideally allowing these cells to express different genes thus reaching a state more similar to that seen *in vivo* compared to 2D models. Cell-matrix interactions mediate several pathways that may be altered in 2D culture, where these interactions

are different. However, the novel 3D system developed herein contains numerous scaffold pores where AMC have a greater opportunity to adhere and reproduce their cell-matrix interactions. Targeted gene expression analysis of adhesion molecules should therefore reveal any alteration in the specific pathways of these molecules between the two culture systems. Using standard culture methods has limited the field of ROM research due to traditional cultures forcing cells to live in an environment not typical of that seen *in vivo*. Therefore, utilizing a culture model that is more similar to that seen *in vivo* is potentially vital to elucidating the mechanisms behind membrane rupture and the future prevention of PPRM by allowing cells to maintain their *in vivo* shape and function. Thus, the hypothesis for Aim 2 is that due to the differences in cellular morphology between the 2D and 3D cell culture models seen in Aim 1, there will be differential gene expression patterns seen in AMC in these environments, due to the response of the cells to their environmental cues.

3.2 Aim 2 To measure the Gene Expression profiles of AMC Grown in 2D and 3D Culture

Aim 2a: Determination of the full transcriptome of AMC grown in traditional 2D culture and in a novel 3D culture system.

Rationale: Since 2D has been shown in previous studies to alter cell culture results, particularly cell-matrix adhesions, it was important to compare adhesion transcripts in the 3D culture system characterized in Chapter 2 to a conventional 2D culture model. The 3D culture system utilized has porosity for an increase in availability for cell adhesions which possibility could result in alterations in gene expression. Therefore, the transcriptome of the amnion may reveal novel functional elements of the genome to further the understanding of these cells and may shed light

on their role in ROM. One way to determine the RNA transcripts is by high-throughput gene sequencing.

RNA-Seq is a newly developed sequencing method in which transcripts can be constructed without a reference strand to precise locations of the single base of transcript boundaries (Wang *et al.* 2009). This method detects and catalogues all RNA (including rare isoforms) from gene structure, splicing patterns, and many other post-transcriptional modifications including gene start sites, 5' and 3' ends (Wang *et al.* 2009). RNA-Seq has been shown to be superior to other sequencing methods partly due to the very low background signal created from non-specific binding that is known to alter results in DNA microarrays (Wang *et al.* 2009). Thus, rendering RNA-Seq a powerful tool in complete evaluation of gene transcripts.

Aim 2b: Measurement of cell adhesion gene expression in AMC grown in 2D and novel 3D culture systems by PCR array and qRT-PCR

Rationale: The comprehensive approach of RNA-seq was designed to evaluate a large number of transcripts between the two different culture conditions of several patients. It is expected that the false discovery rate estimated by the adjusted p value will be fairly large due to the large number of gene evaluated, therefore, other methods of evaluating transcripts should also be employed.

PCR arrays are valuable tools that are able to determine the gene expression levels of a focused panel of pathway specific genes, like extracellular matrix adhesions. However, the results of a PCR array are not definitive as contamination of genomic DNA could result in altered results with false positives. Therefore, once a number of genes with interesting gene expression profiles

are identified, these will be confirmed by qRT-PCR to illustrate the reproducibility of the result. qRT-PCR can also be used to confirm the results obtained by RNA-Seq.

3.3 Materials and Methods

RNA Isolation: AMC were seeded onto 2D 10cm culture dishes and 3D scaffolds at a density of 179,315 and 500,000 respectively. After 7 days in culture, cells were washed twice in 1x PBS then harvested for RNA. 350 μ L RLT (Qiagen, Valencia, CA) buffer was added to the 2D culture plate and the cells removed from the dish with a cell scraper. The RNA was collected from the cells in the 3D model by placing the disc in 700 μ L of RLT buffer for 10 minutes at 40rpm. The RNA isolation was performed following the protocol (cells in culture) from the Qiagen RNeasy kit (Qiagen, Valencia, CA) for both the 2D and 3D cells. A Nanodrop spectrophotometer (NanoVue, GE Healthcare Life Sciences, Pittsburgh PA) was used to determine the RNA concentration and purity based on 260/280 substrate ratios with desired results ≥ 1.8 . Bioanalysis (Agilent 2100 Bioanalyzer, Agilent Technologies, Santa Clara CA) was performed on all RNA samples to ensure adequate RNA integrity (≥ 8) and quantity (0.1-4.0 μ g total) for RNA-Seq library production.

Library Creation and RNA-Seq: At the Beckman Coulter Genomics lab (Danvers, MA), the RNA samples were fragmented chemically with Illumina kit reagents and then underwent reverse transcription, after being primed with hexamers, to cDNA. Second strand cDNA was formed by using the first generated strand as a template while removing the RNA template through PCR. RNA-Seq was then performed using the Illumina sequencing pipeline, which is performed on a flow cell to allow fragment bridge amplification with DNA polymerase. The

DNA fragments were then extended by one fluorescently labeled nucleotide. Each cluster was imaged with a laser over 52 cycles to sequence the entire fragment one base pair at a time. Data was formatted in nucleotide sequences in the fastq format.

RT² Profiler PCR Array: RNA was collected from AMC grown on 2D and 3D as for RNAseq. The creation of cDNA was performed using the RT² First Strand kit (Qiagen, Valencia, CA), generating a genomic DNA mix (250ng RNA, 2μL Buffer GE, and RNase free water for final volume of 10μL) per each patient sample (n=3) and these were heated for 5 minutes at 42°C. The reverse transcription mix was then generated per sample (16μL 5x Buffer BC3, 4μL Control P2, 8μL RE3 Reverse transcriptase mix, and 12μL RNase free water) and 10μL of this reverse transcriptase mix was added to each sample of genomic DNA. Samples were then incubated at 42°C for 15 minutes and then 95°C for 5 minutes. 9μL of RNase free water was added to each sample of newly generated cDNA.

Preparation of the PCR array components was performed by mixing 1350μL of 2x RT²-SYBR Green Mastermix, 102μL of cDNA, and 1248μL of RNase free water. 25μL of each PCR component mix was added to each of the 96 wells of the array. The array (Qiagen, Valencia, CA) was placed in the Applied Biosystems PCR system for 1 cycle at 95°C for 10 minutes to activate the Taq Polymerase and 40 cycles over 15 seconds for 95°C and 1 minute at 60°C.

qRT-PCR: qRT-PCR was performed by generating cDNA from 700 ng of RNA from AMC grown in 2D and 3D culture. A negative RNA control and a water control were also prepared during the reverse transcription procedure. The RNA samples underwent a reverse transcriptase polymerase chain reaction to synthesize cDNA when placed in a thermocycler heated to 37°C for 60 minutes and then 95°C for 5 minutes using 700ng of RNA in 140μL RT with a high capacity RNA to cDNA kit (Applied Biosystems, Grand Island NY). The endogenous expression of the

genes that were chosen to be confirmed were measured in several candidate cell lines; HEK293, MCF-7, WISH, placenta, and AMC, ran with 500ng in an 80 μ L RT. Upon analysis it was determined that relative standard curves (1:10, five points) would be generated with MCF-7 (18s, MMP9 and cadherin 1 (CDH1)) and AMC (connective tissue growth factor (CTGF), Integrin alpha 1 (INTA1) and Fibronectin (FN1)) (Life Technologies, Carlsbad CA). 18s was used as a housekeeping gene to normalize for any difference in RNA starting concentration. Each 20 μ L cDNA sample was added to TaqMan master mix, created by adding per sample to 16 μ L of PCR quality dH₂O, 4 μ L Taqman gene, and 40 μ L of master mix. A new PCR water control generated during the real-time PCR reaction mix generation. A total of 20 μ L of the reaction mix was then placed in PCR plate wells in triplicates. Using the Applied Biosystems PCR system, the PCR plate underwent cycles of 50°C for 2 minutes, 95°C for 10 minutes, and then 40 cycles at 95°C for 15 seconds and 60°C for 1 minute.

Statistical analysis: Statistical analysis was conducted on the PCR array data in collaboration with the Biostatistics Core at University of Hawai'i John A. Burns School of Medicine. The 80 array genes were normalized to the 5 housekeeping genes to minimize starting RNA concentration variation. Linear correlation between two samples compared with a normalized scatterplot matrix, principle component analysis, and hierarchical clustering analysis was completed. Subsequently, comparison of fold changes between 2D and 3D results was performed by paired t-tests to determine differences in expression between the culture conditions for every gene. qRT-PCR results were also analyzed using PRISM. A paired t-test was used to determine significant differences in gene expression between 2D and 3D culture conditions. Values where $p < 0.05$, were considered significant. False discovery rate was calculated for genes by adjusted p value.

3.4 Results

The aim of this chapter was to determine and characterize changes in cellular behavior dictated by the environment within which AMC were grown. Thus, the PCR results were generated to answer the question; is there a difference in cell adhesion gene expression of AMC grown in 2D compared to those grown in 3D culture?

Aim 2a: Determination of the full transcriptome of AMC grown in traditional 2D culture and in a novel 3D culture system.

To evaluate the all of transcripts in AMC that have been grown in 2D and 3D culture, RNA-Seq was the chosen. These studies are ongoing and to date 2 samples have been collected. These samples have been subjected to both nanodrop and full Bioanalysis and have therefore reached the benchmarks for the sequencing process of RNA purity ≥ 1.8 and RNA integrity number greater than 8. However, more AMC from other patients need to be collected, so that a total of 5 patients' patterns of gene expression can be studied.

Aim 2b: Measurement of cell adhesion gene expression in AMC grown in 2D and novel 3D culture systems by PCR array and qRT-PCR

To evaluate differences in the profile of cell adhesion genes in AMC cultured in 2D and 3D, a PCR array was performed. Out of 80 tested cell adhesion genes, only 2 of the genes showed statistically significant differences between the culture methods; collagen type VIII, alpha 1 and Thrombospondin 1, both of which were upregulated in AMC grown in 2D culture compared to 3D (Table 4) with a false discovery rate of 0.037 and 0.732 respectively.

Based on the PCR array results, five genes were chosen for confirmation of gene expression with qRT-PCR (Table 5). Cadherin 1 and connective tissue growth factor were

chosen as they were among the genes that had the highest fold change between the two types of culture. The MMP 9 and fibronectin 1 genes were also chosen for confirmation based on their relevance to fetal membrane research. Lastly, integrin alpha 1 was chosen as a gene for further study as it showed little change between the conditions and because interestingly its expression in the amnion has only been noted once (Malak, Bell 1994). However, before qRT-PCR could be performed, endogenous gene expression for the chosen primers needed to be determined in a variety of cell types for creation of relative standard curves (Table 6). The gene expression levels for the different cell types showed that AMC could be used as an endogenous control for INTA1, CTGF, and FN1 while MCF-7 for MMP9 and CDH1. This was based on the highest endogenous levels of expression for each gene.

Relative gene expression of the 5 chosen genes was performed to determine how robust the PCR array data was as only 3 paired patients' samples were used. The gene expression data generated from the qRT-PCR showed that there were no significant differences between the expression of the target genes in AMC when grown in either 2D or 3D culture (Figure 20).

3.5 Discussion

The purpose of this Aim was to investigate changes in gene expression between AMC grown in 2D compared to those grown in 3D by the evaluation of mRNA levels. This was hypothesized based on the differences in cellular morphology between these conditions noted in Aim 1. The genes chosen for study were focused on ECM components and cell adhesion molecules that might explain the changes in cell geometry and adhesions on different planes. It is these cellular adhesions that dictate the translation of information between the cells and their

surrounding environment (Cukierman *et al.* 2001), and are also the key regulators for the integrity of the ECM of the fetal membranes and their rupture (Bryant-Greenwood 1998).

The cell adhesion PCR array chosen, used a relatively small amount of RNA which allowed subsequent experiments employing the same patient's sample. Among the 80 genes tested, only 2 resulted in significant differences between AMC in 2D and 3D: collagen VIII and thrombospondin 1, which were upregulated 3 fold in 2D (Table 4). The expression of the anti-angiogenesis gene thrombospondin 1 is consistent with the avascular nature of the amnion, but the difference in expression between 2D and 3D was surprising. While known to be expressed in AEC at term, thrombospondin 1 is thought to be only rarely expressed in term AMC (Hao *et al.* 2000). The reasons for this are unknown, but gestational age may be a factor. Although unclear from the data collected, the expression of thrombospondin 1 in 2D culture may be indicative their epithelial-like morphology and gained polarity in a flat culture system.

The difference in expression of collagen VIII was also surprising as it is known to have a role in angiogenic remodeling for subendothelial ECM (Shuttleworth 1997; Plenz *et al.* 2003), but it has not been identified in previous studies of the collagen profile of the amnion (Bryant-Greenwood 1998; Niknejad *et al.* 2008). The fact that collagen VIII is not a known amnion collagen does not preclude it from influencing AMC function, but its role is yet to be elucidated. Its increased expression in 2D culture could reflect the acquired AEC phenotype of AMC in attempt to create a basement membrane. It is still also unclear as to which level of AMC expression of collagen VIII is a true representation of the fetal membranes. To determine if indeed collagen VIII is a constituent of the amnion, evaluation by immunohistochemistry and western blotting on freshly collected tissue could yield an answer. Collagen VIII in the amnion could interact with previously discovered, vascular endothelial growth factor (VEGF), and

contribute to changes in the permeability of the placental amnion (Astern *et al.* 2013). To evaluate if collagen VIII is colocalized with VEGF, future studies could include immunohistochemistry on regions of fetal membrane sections as well as the measurement of protein and gene expressions to acquire a full understanding of its potential role in the amnion.

To confirm the array results, 5 genes were chosen for qRT-PCR (Table 5). However, collagen VIII and thrombospondin 1 were not amongst those 5 genes because the preliminary analysis of the arrays was performed with an incomplete set of data. From the single complete patient data collected after the first PCR array run, the expression of collagen VIII did not appear to have a significant change. This reflects the underpowered nature of this study and more patient samples will be needed for a solid comparison.

The qRT-PCR data reflected the PCR array data, in the sense that the 5 genes chosen showed no significant difference between 2D and 3D culture environments over a 7 day culture period (Figure 20). However, this does not mean AMC in the two culture systems are void of any variation, as gene expression may not give an accurate picture of the level of biologically active protein level. Therefore, future work will focus on the differential protein expression of AMC in 2D and 3D by utilizing western blot, immunocytochemistry, or immunohistochemistry techniques to obtain a more comprehensive understanding of how these cells behave in the different culture environments.

To properly evaluate gene expression, certain factors should be considered to ensure that the amplification seen is a true representation of the level of gene expression in the sample. This is due to the potential of numerous steps in the PCR process; from primer design, amount of RNA added, and chosen reporter dye that can lead to false positives. It is important for primers to be uncomplimentary to themselves and each other while within an adequate length to proper

annealing to the desired strand of DNA. To ensure that the newly designed primer will not bind to other DNA sequences, there are software sequence databases, like BLAST, that can be used to rule out any non-targeted binding of the primer sequence. Internal controls for PCR involve the use of various housekeeping genes, which encode proteins that are endogenously expressed in cells, which often include actin, histones, and ribosomal proteins. The use of only a single housekeeping gene can lead to large changes in expression data if the level of that gene expression change between experimental conditions. Therefore, it is important to use numerous housekeeping genes in PCR for data normalization.

The expansion of the work in this Aim should include the detection of translated proteins, secreted proteins, and enzyme activity, to uncover any cellular behavior differences of AMC grown in 2D and 3D. It is also evident that the completion of the ongoing RNA-Seq experiments may be essential for the identification of any potential differential expression between AMC in the two culture systems beyond ECM and cell adhesion molecules. However, large numbers of sequenced genes can also result in false positives that have to be confirmed, and repeatable, using other methods. The work in Aim 2 only showed significant gene expression differences with the PCR array between 2D and 3D, but these results will need to be confirmed with other methods so that solid conclusions can be made. Therefore, further work is needed to determine if there are any changes to cellular function that are a result of the alteration in AMC morphology seen in Aim 1.

Expression (fold change)				Paired T-test	
2D/3D	log(FC)	Regulated	3D/2D	P-values	Gene
3.48216	0.54185	Up	0.28718	0.24977	ADAM metalloproteinase with thrombospondin type 1 motif, 1
5.94224	0.77395	Up	0.16829	0.09976	ADAM metalloproteinase with thrombospondin type 1 motif, 13
44.34093	1.64680	Up	0.02255	0.90254	ADAM metalloproteinase with thrombospondin type 1 motif, 8
1.18618	0.07415	Up	0.84304	0.40450	CD44 molecule
15.07973	1.17839	Up	0.06631	0.09691	Cadherin 1, type 1, E-cadherin (epithelial)
2.04425	0.31053	Up	0.48918	0.35692	C-type lectin domain family 3, member B
2.26630	0.35532	Up	0.44125	0.55022	Contactin 1
4.13892	0.61689	Up	0.24161	0.19611	Collagen, type XI, alpha 1
0.86325	-0.06386	down	1.15841	0.91641	Collagen, type XII, alpha 1
1.00330	0.00143	Up	0.99671	0.58106	Collagen, type XIV, alpha 1
0.42866	-0.36789	down	2.33286	0.33343	Collagen, type XV, alpha 1
1.99022	0.29890	Up	0.50246	0.62596	Collagen, type XVI, alpha 1
1.77799	0.24993	Up	0.56243	0.38864	Collagen, type I, alpha 1
1.99305	0.29952	Up	0.50174	0.10634	Collagen, type IV, alpha 2
1.21061	0.08300	Up	0.82603	0.66537	Collagen, type V, alpha 1
1.21636	0.08506	Up	0.82212	0.30168	Collagen, type VI, alpha 1
0.75215	-0.12369	down	1.32952	0.08230	Collagen, type VI, alpha 2
1.29999	0.11394	Up	0.76924	0.64177	Collagen type VII, alpha 1
2.91019	0.46392	Up	0.34362	0.00040	Collagen type VIII, alpha 1
11.80044	1.07190	Up	0.08474	0.11041	Connective tissue growth factor
1.84329	0.26559	Up	0.54251	0.49885	Catenin (cadherin-associated protein), alpha 1 102kDa
1.59221	0.20200	Up	0.62806	0.42010	Catenin (cadherin-associated protein), alpha 1 88kDa

1.54130	0.18789	Up	0.64880	0.49183	Catenin (caderin-associated protein), delta 1
1.00218	0.00095	Up	0.99782	0.66023	Catenin (caderin-associated protein), delta 2 (neural plakophilin-related arm-repeat protein)
1.10848	0.04473	Up	0.90214	0.54836	Extracellular matrix protein 1
1.01954	0.00840	Up	0.98083	0.84778	Fibronectin 1
4.58938	0.66175	Up	0.21789	0.98848	Hyaluronan synthase 1
1.06743	0.02834	Up	0.93683	0.58131	Intercellular adhesion molecule 1
1.01214	0.00524	Up	0.98801	0.65180	Integrin, alpha 1
0.40685	-0.39057	down	2.45792	0.95155	Integrin, alpha 2 (CD49B, alpha 2 subunit of VLA-2 receptor)
2.18208	0.33887	Up	0.45828	0.35631	Integrin, alpha 3 (antigen CD49C, alpha 3 subunit of VLA-3 receptor)
2.45818	0.39061	Up	0.40681	0.23227	Integrin, alpha 4 (antigen CD49D, alpha 4 subunit of VLA-4 receptor)
2.90561	0.46324	Up	0.34416	0.62213	Integrin, alpha 5 (fibronectin receptor, alpha polypeptide)
3.05115	0.48446	Up	0.32775	0.05318	Integrin, alpha 6
3.15168	0.49854	Up	0.31729	0.49969	Integrin, alpha 7
4.17038	0.62018	Up	0.23979	0.45644	Integrin, alpha 8
373.33082	2.57209	Up	0.00268	0.33334	Integrin, alpha L (antigen CD11A (p180), lymphocyte function-associated antigen 1; alpha polypeptide)
1.06026	0.02541	Up	0.94316	0.86067	Integrin, alpha V (vitronectin receptor, alpha polypeptide, antigen CD511)
1.59135	0.20176	Up	0.62840	0.46410	Integrin, beta 1 (fibronectin receptor, beta polypeptide, antigen CD29 includes MDF2, MSK12)
3.97774	0.59964	Up	0.25140	0.18646	Integrin, beta 2 (complement component 3 receptor 3 and 4 subunit)
2.66978	0.42648	Up	0.37456	0.80549	Integrin, beta 3 (platelet glycoprotein IIIa, antigen CD61)
3.46501	0.53970	Up	0.28860	0.35022	Integrin, beta 4
0.94647	-0.02389	down	1.05656	0.90186	Integrin, beta 5
1.38661	0.14196	Up	0.72118	0.44920	Kallmann syndrome 1 sequence
1.07767	0.03249	Up	0.92793	0.90034	Laminin, alpha 1
1.74761	0.24244	Up	0.57221	0.95674	Laminin, alpha 2
3.16021	0.49972	Up	0.31643	0.18532	Laminin, alpha 3
1.43313	0.15629	Up	0.69777	0.31893	Laminin, beta 1

9.12846	0.96040	Up	0.10955	0.33368	Laminin, beta 3
1.81013	0.25771	Up	0.55245	0.21920	Laminin, gamma 1 (formally LAMB2)
0.10160	-0.99309	down	9.84212	0.21037	Matrix metalloproteinase 1 (interstitial collagenase)
0.68979	-0.16128	down	1.44972	0.73555	Matrix metalloproteinase 10 (stromelysin 2)
0.27523	-0.56030	down	3.63333	0.49815	Matrix metalloproteinase 11 (stromelysin 3)
0.68952	-0.16145	down	1.45028	0.90712	Matrix metalloproteinase 12 (macrophage elastase)
0.18675	-0.72874	down	5.35472	0.19615	Matrix metalloproteinase 13 (collagenase 3)
0.79039	-0.10216	down	1.26520	0.92617	Matrix metalloproteinase 14 (membrane-inserted)
98.72840	1.99444	Up	0.01013	0.44099	Matrix metalloproteinase 15 (membrane-inserted)
4.78388	0.67978	Up	0.20904	0.77842	Matrix metalloproteinase 16 (membrane-inserted)
0.59461	-0.22577	down	1.68179	0.49726	Matrix metalloproteinase 2 (gelatinase A, 72kDa gelatinase, 72kDa type IV collagenase)
0.26369	-0.57890	down	3.79229	0.73608	Matrix metalloproteinase 3 (stromelysin, 1, progelatinase)
8.76382	0.94269	Up	0.11411	0.96092	Matrix metalloproteinase 7 (matrilysin, uterine)
91.77325	1.96272	Up	0.01090	0.99713	Matrix metalloproteinase 8 (neutrophil collagenase)
1.62244	0.21017	Up	0.61636	0.76891	Matrix metalloproteinase 9 (gelatinase B, 92kDa gelatinase, 92kDa type IV collagenase)
1.52753	0.18399	Up	0.65465	0.33017	Neural cell adhesion molecule 1
138.59868	2.14176	Up	0.00722	0.58856	Platelet/endothelial cell adhesion molecule
372.98634	2.57169	Up	0.00268	0.48616	Selectin L
0.18114	-0.74197	down	5.52046	0.12419	Selectin P (granule membrane protein 140kDa, antigen CD62)
1.84254	0.26542	Up	0.54273	0.91681	Sarcoglycan, epsilon
2.20579	0.34357	Up	0.45335	0.63577	Secreted protein, acidic, cysteine-rich (osteonectin)
1.64815	0.21700	Up	0.60674	0.43337	Spastic paraplegia 7 (pure and complicated autosomal recessive)
0.41653	-0.38036	down	2.40082	0.20988	Secreted phosphoprotein 1
2.68774	0.42939	Up	0.37206	0.06207	Transforming growth factor, beta-induced, 68kDa
3.43496	0.53592	Up	0.29112	0.04122	Thrombospondin 1
0.79605	-0.09906	down	1.25620	0.98782	Thrombospondin 2
4.67356	0.66965	Up	0.21397	0.23835	Thrombospondin 3

0.55693	-0.25420	down	1.79555	0.30415	TIMP metalloproteinase inhibitor 1
2.03908	0.30943	Up	0.49042	0.17645	TIMP metalloproteinase inhibitor 2
2.30657	0.36297	Up	0.43354	0.20645	TIMP metalloproteinase inhibitor 3
0.39346	-0.40510	down	2.54159	0.36129	Tenascin C
0.26983	-0.56891	down	3.70601	0.27480	Vascular cell adhesion molecule 1
1.26433	0.10186	Up	0.79093	0.65810	Versican
5.77217	0.76134	Up	0.17325	0.06415	Vitronectin

Table 4. Extracellular matrix cell adhesion array results from AMC grown in 2D vs 3D culture. Fold changes greater than 2 and significant differences between the conditions (p values <0.05) are highlighted in grey.

Gene	Fold Change	P value
Cadherin 1, type 1, E-cadherin (epithelial)	15.07973	0.09691
Connective tissue growth factor	11.80044	0.11041
Fibronectin 1	1.01954	0.84778
Integrin, alpha 1	1.01214	0.65180
Matrix metalloproteinase 9 (gelatinase B, 92kDa gelatinase, 92kDa type IV collagenase)	1.62244	0.76891

Table 5. Genes chosen from PCR array data to confirm with qRT-PCR. Fold change shown is upregulation in 2D compared to 3D culture.

Cell Type	Gene Ct Value				
	INTA1	CTGF	FN1	MMP9	CDH1
HEK 293	29.47724215	30.06735675	28.00234413	32.65513738	26.48741913
MCF-7	36.53753026	33.3223877	26.47976176	30.86471176	19.36621857
WISH	24.70076752	31.53813108	27.81044769	35.73825963	30.0694383
Placenta	25.80386734	24.41281509	21.47577731	30.99280421	23.8522447
AMC 2D	25.14332008	20.0428594	18.60658073	36.64402262	35.55251567

Table 6. Endogenous gene expression evaluation of gene primers in 5 different cell types.

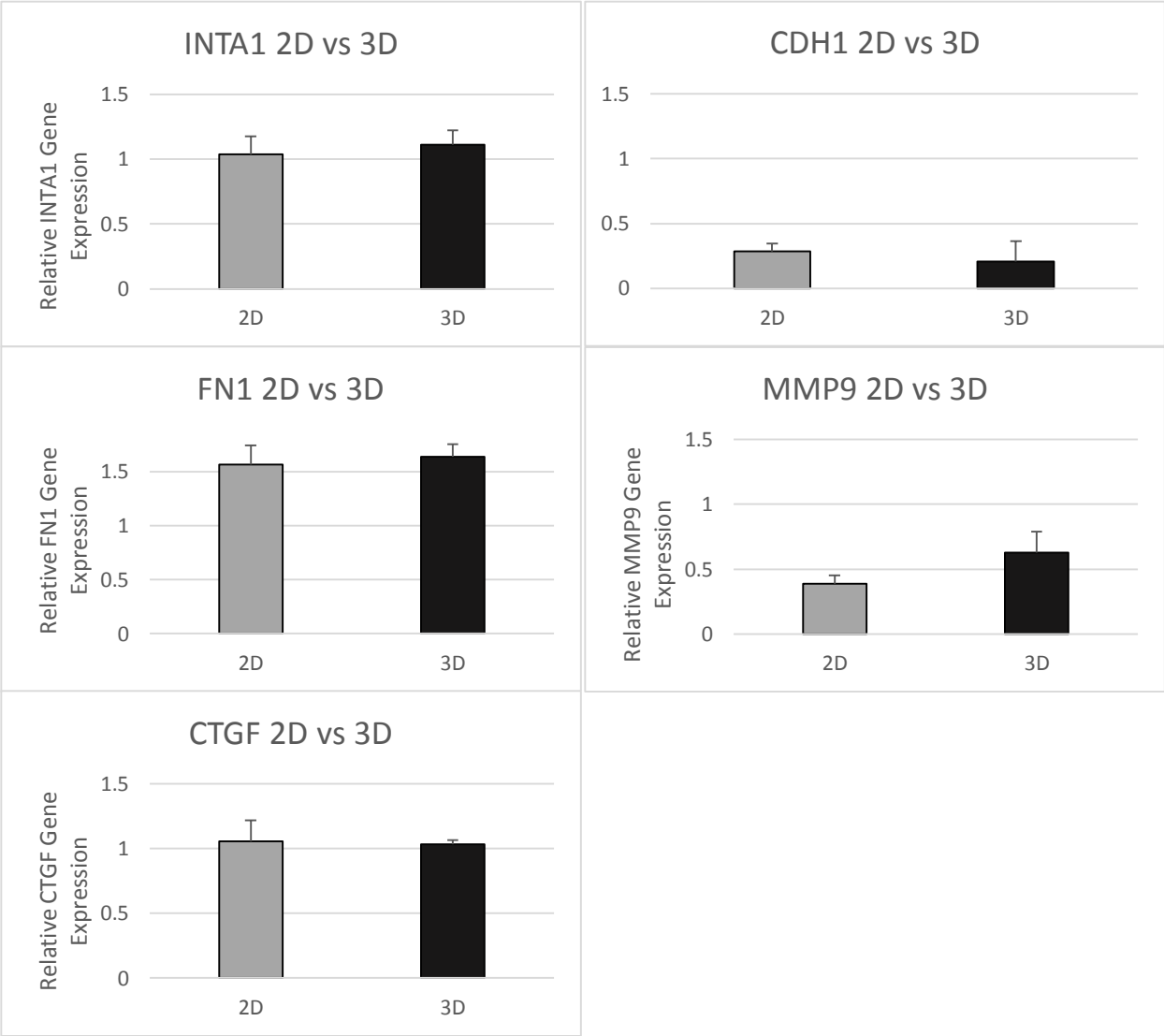


Figure 20. Relative gene expression of INTA1, FN1, CTGF, CDH1, and MMP9 in AMC grown in 2D and 3D culture by qRT-PCR.

Chapter 4. Discussion

The overall goal for this thesis was to construct and test a novel 3D culture system for AMC using an inert substance that would allow the cells to develop adhesions similar to those that would be seen in *in vivo* conditions. It was thought that such a model would improve the accuracy of culture conditions, compared to the traditional 2D culture model. This AMC 3D model was conceived as a potentially better way to study the amnion, with the future application of using it to understanding the mechanisms of ROM. Thus the behavior of AMC within 2D and 3D environmental conditions was evaluated to determine if some of the limitations of 2D cultures could be overcome.

The polystyrene scaffold culture system was validated based on cell density, proliferation, migration, changes in cellular morphology, contamination, and cell survival in Aim 1. The results demonstrated that the AMC were able to adhere to the scaffold in a 3-dimensional fashion while proliferating and migrating throughout, with low levels of cytotoxicity. The most conspicuous change was that the AMC morphology changed from a flattened, hypertrophic appearance in 2D to the thin spindle shape seen in 3D. This supports the theory that cellular geometry governs cellular adhesion and some cellular functions (Kilian *et al.* 2010). The contamination of AMC with AEC could alter cell signaling and will limit any conclusions of AMC behavior in this study, as the 3D system as is, would be most useful as a sole AMC model to study their specific expression profiles in the mesenchymal layer. Ongoing work aims to determine if AEC identification in this model is due to contamination or cellular differentiation. The addition of further study of the cells' viability would also help to ensure confidence that this model is a true representation of the amnion mesenchymal layer. Experiments designed to study changes in cellular behavior in the novel 3D model showed that out of the 30 genes evaluated by

gene array, only 2 genes showed significant difference in 2D compared to 3D. Therefore, future work will focus on determining the role of these genes, collagen VIII and thrombospondin 1, as well as the confirmation of the differential expression on other cellular levels such as protein translation, protein secretion, and enzyme activity.

The culture model created in this study was the first attempt to place AMC into a 3D environment for research specific to ROM. However, future studies with this model are not limited to studying the AMC layer. Concepts of ROM can be elucidated with the addition of a co-culture technique with AEC to give a full understanding of the entire amnion and how the addition of AEC changes AMC behavior. To continue to build this model and create an environment more similar to *in vivo*, various collagens, particularly type I and III, can be introduced to AMC within the 3D culture for the evaluation of how they remodel their extracellular matrix. Even more crucial to ROM research is that the model can include the introduction of infection and the induction of inflammation so that it will be possible to be able to study the three main mechanisms for early membrane rupture in one controlled environment, which is currently not possible.

The novel 3D AMC model can be a useful tool for uncovering the changes in AMC behavior in correlation to gestation. At the end of gestation, AMC stop proliferating, assumedly to aid in the normal weakening processes of the fetal membranes (Bryant-Greenwood 1998), but little is known about the cellular cues involved with this modification. The cells used in this thesis were collected from near term tissue between a 39-42 weeks gestational period, but upon IRB approval, earlier tissues can be collected to evaluate AMC behavior between preterm and near term tissues. This can allow insight into the normal changes of AMC *in vivo* through gestation leading to fetal membrane rupture.

The effect certain drugs have on the amnion, particularly ones used to remedy PPRM, can also be studied with the 3D system generated. One common treatment of PPRM involves the administration of corticosteroids for accelerating neonatal organ development, but it increases the likelihood of perinatal infection (Mercer 2004). Another treatment for PPRM is the daily vaginal administration of progesterone, however, this has uncertain long-term repercussions for the developing baby. The use of these therapies is controversial, and overall effects on the amnion and the baby are unclear. Therefore, this 3D model could be used to reveal the corticosteroid and progesterone effects on the amnion and identify potential dangers for the developing baby encapsulated within. The effect other drug therapies have on the amnion can also be evaluated using this 3D system since there are many ethical constraints around determining their effect on pregnant women and developing fetuses. In support of this, previous studies have demonstrated differences in cellular metabolism when cells are grown in 2D compared to 3D culture, resulting in altered reactions to drug therapies (Santini *et al.* 2003). Due to the changes in cell metabolism, the evaluation of drugs on AMC in this 3D system could reshape the way certain therapies are used to treat PPRM and other various ailments affecting pregnant women.

Studies focusing around AMC adhesions can also be done with the Alvetex scaffold, due to its porosity, allowing the cells to retain fibroblast-like attachments. Imaging from Aim 1 demonstrated that AMC are able to make multiple adhesions and suspend within a single pore, forcing adhesions on the entire peripheral surfaces. Despite the fact that gene expression evaluation showed no differences in cellular adhesion molecules, the particular location of the adhesion can alter. This phenomenon was noted in a previous study where fibroblasts' focal and fibrillary adhesions colocalized with fibronectin when placed in 3D culture, which was contrary

to 2D culture (Cukierman *et al.* 2001). Further research involving the characterization of AMC adhesions in the novel 3D system compared to 2D could provide information regarding the potential differences in cellular behavior, as cellular morphology and cell adhesions have roles in governing cellular function.

Further evaluation and validation of the novel 3D system needs to be completed before other applications can be studied. Particular importance should focus on isolating a pure AMC population for the assurance of genuine AMC behaviors that are not altered from a mixed cell population. While the degree of apoptosis and necrosis is presumed to be low, the actual rates need to be determined as they can have an effect on the longevity and viable use of the culture system. The PCR array and qRT-PCR experiments did not result in many significant gene expression variations of the ECM and adhesion molecules, however, the completion of RNA-Seq will unveil the full transcriptome of AMC within the two culture systems and determine if there are any other differential expressions. The result of little significant differences in gene expression, does not mean that there are none, as those differences may rest on the protein level, or be based on location, as documented with other fibroblast cell adhesions (Cukierman *et al.* 2001).

The main focus of this thesis was to create a 3D cell culture model for AMC that is improved upon 2D culture in terms of its ability to provide an environment that is more comparable to *in vivo* amnion conditions. This work demonstrated that AMC are viable in the inert polystyrene scaffold, with clear morphological changes compared to 2D cultured AMC. Evaluations of cell survival and a small disparity in gene expression identified the complexity of the future endeavors needed to be completed for the full validation of this 3D model. Overall, the

generation of a novel 3D system was a large leap forward in creating a 3D model with primary purpose of researching the amnion and the mechanisms of its rupture.

REFERENCES

- Alberts, B. J. (2008). *Molecular Biology of the Cell*. Garland Science, Taylor & Francis Group.
- Arikat, S. M. (2006). Separation of amnion from corioid decidua is an integral event to the rupture of normal term fetal membranes and constitutes a significant component of the work required. *American Journal of Obstetrics and Gynecology*, 194(1), 211-217.
- Astern, J. C.-W. (2013). Pre-B cell colony enhancing factor (PBEF/NAMPT/Visfatin) and vascular endothelial growth factor (VEGF) cooperate to increase permeability of the human placental amnion. *Placenta*, 42-49.
- Baker, B. C. (2012). Deconstructing the third dimension- how 3D culture microenvironments alter cellular cues. *Journal of Cell Science*, 3015-3024.
- BBC News. (2007, December 13). *BBC News*. Retrieved from Curvier spines aid pregnant women: <http://news.bbc.co.uk/2/hi/health/7137104.stm>
- Belser, J. e. (2013, May). Pathogenesis Transmissibility, and Ocular Tropism of a Highly Pathogenic Avian Influenza A (H7N3) Virus Associated with Human Conjunctivitis. *J Virol*, 87(10), 5746-5754.
- Bilic, G. H.-K. (2005). Human Preterm Amnion Cells Cultured in 3-Dimensional Collagen I and Fibrin Matrices for Tissue Engineering Purposes. *American Journal of Obstetrics & Gynecology*(193), 1724-1732.
- Bryant-Greenwood, G. (1998). The Extracellular Matrix of the Human Fetal Membranes: Structure and Function. *Placenta*(19), 1-11.
- Bryant-Greenwood, G. M. (2000). Human Fetal Membranes: Their Preterm Premature Rupture. *Biology of Reproduction*(63), 1575-1579.
- Casey, M. M. (1996). Interstitial Collagen Synthesis and Processing in Human Amnion: A Property of the Mesenchymal Cells. *Biology of Reproduction*(55), 1253-1260.
- Centers for Disease Control and Prevention. (n.d.). *Preterm Birth*. Retrieved June 9, 2015, from <http://www.cdc.gov/reproductivehealth/maternalinfanthealth/pretermbirth.htm>
- Challis, J. (2000). Mechanism of Parturition and Preterm Labor. *Obstetrical and Gynecological Survey*, 55(10), 650-660.
- Chua, W. O. (2009). Do we know the strength of the chorioamnion? A critical review and analysis. *European Journal of Obstetrics & Gynecology and Reproductive Biology*(144s), s128-s133.
- Crowther, C. e. (2002). Magnesium Sulphate for Preventing Preterm Birth in Threatened Preterm Labour. *The Cochrane Library*.
- Cukierman, E. P. (2001, November). Taking Cell-Matrix Adhesions to the Third Dimension. *Science*, 294, 1708-1712.

- Cukierman, E. P. (2002). Cell Interactions with Three-Dimensional Matrices. *Current Opinion in Cell Biology*(14), 633-639.
- Drummond, I. G. (1997). Immortal, developmentally arrested human fetal kidney cell lines created by retroviral expression of human papilloma virus E6 and E7. *Exp Nephrol*(5), 390-398.
- Elmore, S. (2007). Apoptosis: A Review of Programmed Cell Death. *Toxicol Pathol.*, 35(4), 495-516.
- Elovitz, M. M. (2004, December). Animal models of preterm birth. *TRENDS in Endocrinology and Metabolism*, 15(10), 479-487.
- Elsdale, T. B. (1972). Collagen Substrata for Studies on Cell Behavior. *Cell Biology*(54), 626-637.
- Ewald, A. B. (2008). Collective Epithelial Migration and Cell Rearrangements Drive Mammary Branching Morphogenesis. *Dev. Cell*, 14(4), 570-581.
- Falzone, N. H. (2009). Comparison between propidium iodide and 7-amino-actinomycin-D for viability assessment during flow cytometric analysis of the human sperm acrosome. *First Journal of Andrology*, 20-26.
- Goldenberg, R. C. (2008, January 5). Epidemiology and Causes of Preterm Birth. *The Lancet*, 371, 75-84.
- Golstein, P. K. (2006, Jan). Cell Death by Necrosis: Towards a Molecular Definition. *Trends Biochem Sci.*, 32(1), 37-43.
- Grinnell, F. (2003). Fibroblast biology in three-dimensional collagen matrices. *TRENDS in Cell Biology*, 13(5).
- Hao, Y. e. (2000). Identification of Antiangiogenic and Antiinflammatory Proteins in Human Amniotic Membrane. *Cornea*, 348-352.
- Hayes, D. S. (2010, November). Premature Birth Fact Sheet.
- Henderson, W. G. (1953, December). The use of culture virus in the preparation of foot-and-mouth disease vaccine. *JHyg (Lond)*, 51(4).
- Hieber, A. D.-G. (1997). Detection of Elastin in the Human Fetal Membranes: Proposed Molecular Basis for Elasticity. *Placenta*(18), 301-312.
- Hirai, A. H. (2013, Nov). Excess infant mortality among Native Hawaiians: identifying determinants for preventive action. *Journal of Public Health*, 103(11), 88-95.
- Hu, H. H. (2014). Deep Sequencing Reveals a Novel Class of Bidirectional Promoters Associated with Neuronal Genes. *BMC Genomics*. doi:doi:10.1186/1471-2164-15-457
- Institute of Medicine (US) Committee on Understanding Premature Birth and Assuring Healthy. (2007). *Preterm Birth: Causes, Consequences, and Prevention*. (R. B. Behrman, Ed.) Retrieved 2015, from <http://www.nap.edu/catalog/11622/preterm-birth-causes-consequences-and-prevention>
- Khwad, M. S. (2005). Term Human Fetal Membranes Have a Weak Zone Overlying the Lower Uterine Pole and Cervix Before Onset of Labor. *Biology of Reproduction*(72), 720-726.

- Kilian, e. a. (2010). Geometric cues for directing the differentiation of mesenchymal stem cells. *PNAS*, 4872-4877.
- Kim, C. R. (2011). *The Placenta in Preterm Prelabor Rupture of Membranes and Preterm Labor* (First ed.).
- Knight, E. M. (2011). Alvetex: Polystyrene Scaffold Technology for Routine Three Dimensional Cell Culture. (J. W. Haycock, Ed.) *3D Cell Culture: Methods and Protocols*(695), 323-340.
- Knight, E. P. (2014). Advances in 3D Cell Culture Technologies Enabling Tissue-Like Structures to be Created in vitro. *Journal of Anatomy*, 10, 1111/joa.122257.
- König, J. e. (2014). Amnion-derived mesenchymal stromal cells show a mesenchymal-epithelial phenotype in culture. *Cell Tissue Bank*, 193-198.
- Liu, Y. S.-L. (2004). Novel Role for Netrins in Regulating Epithelial Behavior During Lung Branching Morphogenesis. *Curr Biol*, 14(10), 897-905.
- Ludmir, J. S. (2000). Anatomy and Physiology of the Uterine Cervix. *Clinical Obstetrics and Gynecology*, 433-439.
- Malak, T. B. (1994). Differential expression of the integrin subunits in human fetal membranes. *Journal of Reproduction and Fertility*, 269-276.
- March of Dimes. (2015). *March of Dimes Prematurity Campaign*. Retrieved March 06, 2015, from <http://www.marchofdimes.org/mission/prematurity-campaign.aspx>
- Maruyama, N. e. (2013). Hypoxia enhances the induction of human amniotic mesenchymal side population cells into vascular endothelial lineage. *Int J Mol Med.*, 315-322.
- Mehta, G. H. (2012). Opportunities and challenges for use of tumor spheroids as models to test drug delivery and efficacy. *Journal Control Release*(164), 192-204.
- Mercer, B. (2004). Chapter 47. Preterm Premature Rupture of the Membranes. *Gynecology and Obstetrics*. Lippincott Williams & Wilkins. Retrieved 2015, from <https://www.glowm.com/resources/glowm/cd/pages/v2/v2c047.html>
- Mihu, C. e. (2009). Isolation and Characterization of Mesenchymal Stem Cells from the Amniotic Membrane. *Romanian Journal of Morphology and Embryology*, 50(1), 73-77.
- Mortimer, G. H. (1985, May). A Role for Amniotic Epithelium in Control of Human Parturition. *Lancet*, 1074-1075.
- Niknejad, H. e. (2008). Properties of the Amniotic Membrane for Potential Use in Tissue Engineering. *European Cells and Materials*, 88-99.
- O'Brien, M. B. (1995). Comparison of Cell Viability Probes Compatible With Fixation and Permeabilization for Combined Surface and Intracellular Staining in Flow Cytometry. *Cytometry*, 243-255.
- Parolini, O. A. (2008). Concise Review: Isolation and Characterization of Cells from Human Term Placenta: Outcome of the First International Workshop on Placenta Derived Stem Cells. *Stem Cells*(26), 300-311.

- Patrinios, M. (2002). Chapter III.4. High Risk Pregnancy. In U. o. Department of Pediatrics, *Case Based Pediatrics for Medical Students and Residents*.
- Pledimonte, G. B. (1982). Effect of Cell Density on Growth Rate and Amino Acid Transport in Simian Virus 40-transformed 3T3 Cells. *Cancer Research*(42), 4690-4693.
- Plenz, G. e. (2003). Vascular collagens: spotlight on the role of type VIII collagen in arterogenesis. *Atherosclerosis*, 1-11.
- Qiao, J. S. (1999). Branching Morphogenesis Independent of Mesenchymal-Epithelial Contact in the Developing Kidney. *Proc. Natl. Acad. Sci. USA*(96), 7330-7335.
- Rampersad, R. C.-Z. (2011). Development and Anatomy of the Human Placenta. In *The Placenta: From Development to Disease* (First ed., pp. 19-26).
- Reinnervate. (2014). *Propagation of Human Pluripotent Stem Cells in Three Dimensional Culture Using Alvetex Strata*. Retrieved from <http://reinnervate.com/science-technical-resources/application-notes/propagation-human-pluripotent-stem-cells-three-dimensional-culture-using-alvetex-strata/>
- Reinnervate. (2015). *Formation of Mesenchymal Tissues in Alvetex Scaffold Derived From Stem Cells and Established Cell Lines*. Retrieved June 14, 2015, from <http://reinnervate.com/science-technical-resources/application-notes/formation-of-mesenchymal-tissues-in-alvetexscaffold-derived-from-stem-cells-and-established-cell-lines/>
- Reinnervate ReproCell. (n.d.). *Example protocol for the Culture of the 3T3 Cell Line on Alvetex Scaffold in Well Plate and Well Insert Formats*. Retrieved July 19, 2015, from <http://reinnervate.com/using-alvetex/protocols/3t3-cell-line-on-alvetex-scaffold-well-plate-and-insert-formats/>
- Reti, N. L. (2007, May). Why do membranes rupture at term? Evidence of increased cellular apoptosis in the supracervical fetal membranes. *American Journal of Obstetrics & Gynecology*, 196(5), 484.e1=484.e10.
- Rienzo, M. C. (2014, August 15). RNA-Seq for the Identification of Novel Mediator Transcripts in Endothelial Progenitor Cells. *Gene*, 98-105.
- Rodriguez-Fuentes, N. e. (2015, February). Isolation of Human Mesenchymal Stem Cells and their Cultivation on the Porous Bone Matrix. *Journal of Visualized Experiments*(96).
- Roizen, J. A. (2008). Preterm Birth Without Progesterone Withdrawal in 15-Hydroxyprostaglandin Dehydrogenase Hypomorphic Mice. *Mol. Endocrinol.*, 22(1), 105-112.
- Rowe, T. K. (1997). Tissue inhibitor of metalloproteinase-1 and tissue inhibitor of metalloproteinase-2 expression in human amnion mesenchymal and epithelial cells. *American Journal of Obstetrics & Gynecology*, 915-921.
- Sadler, T. (2012). *Langman's Medical Embryology* (Twelfth ed.).
- Santini, M. R. (2003). MG-63 human osteosarcoma cells grown in monolayer and as three-dimensional tumor spheroids present a different metabolic profile: a 1H NMR study. *FEBS Letters*, 557, 148-154.

- Shamir, E. E. (2014). Three-dimensional organotypic culture: experimental models of mammalian biology and disease. *Nature Reviews: Molecular Cell Biology*(15), 647-664.
- Sharma, R. B. (2013). Epidermal-like architecture obtained from equine keratinocytes in three-dimensional cultures. *Journal of Tissue Engineering and Regenerative Medicine*.
- Shuttleworth, C. (1997). Type VIII Collagen. *Int. J. Biochem. Cell Biol.*, 1145-1148.
- Sung, K. S. (2013). Understanding the Impact of 2D and 3D Fibroblast Cultures on In Vitro Breast Cancer Models. *PLoS ONE*, 8(10). doi:10.1371/journal.pone.0076373
- U.S. Department of Health and Human Services, Health Resources and Services Administration, Maternal and Child Health Bureau. (2013). Retrieved 2015, from Child Health USA 2013: <http://mchb.hrsa.gov/chusa13/perinatal-health-status-indicators/p/preterm-birth.html>
- United Health Foundation. (2015). *America's Health Rankings - Preterm Birth*. Retrieved 2015, from www.americashealthrankings.org/HI/preterm
- Vergani, L. G. (2004). Modifications of chromatin structure and gene expression following induced alterations of cellular shape. *The International Journal of Biochemistry & Cell Biology*(36), 1447-1461.
- Wang, Z. G. (2009). RNA-Seq: a revolutionary tool for transcriptomics. *Nat Rev Genet*, 57-63.
- Weaver, V. e. (2002). β 4 integrin-dependent formation of polarized three-dimensional architecture confers resistance to apoptosis in normal and malignant mammary epithelium. *Cancer Cell*, 205-216.
- Welsh, T. H. (2014, August). Progesterone Receptor Expression Declines in the Guinea Pig Uterus during Functional Progesterone Withdrawal and in Response to Prostaglandins. *PLOS ONE*, 9(8).
- Werner, E. e. (2011). Universal Cervical-Length Screening to Prevent Preterm Birth: a Cost-Effectiveness analysis. *Ultrasound in Obstetrics & Gynecology*, 32-37.
- Xu, P. A. (2002). Expression of Matrix Metalloproteinase (MMP)-2 and MMP-9 in Human Placenta and Fetal Membranes in Relation to Preterm and Term Labor. *The Journal of Clinical Endocrinology & Metabolism*, 1353-1361.
- Zhao, H. L. (2014). Whole Transcriptome RNA-Seq Analysis: Tumorigenesis and Metastasis of Melanoma. *Gene*, 548, 234-243.